UNVERSITÀ DEGLI STUDI DI PADOVA

Sede Amministrativa: Università degli Studi di Padova
Dipartimento di Scienze Biomediche Sperimentali

SCUOLA DI DOTTORATO DI RICERCA IN BIOSCIENZE
INDIRIZZO: BIOLOGIA CELLULARE
CICLO XXI

Studies of Botulinum Neurotoxins Mechanism of Action

Direttore della Scuola: Ch.mo Prof. Tullio Pozzan
Supervisore: Ch.mo Prof. Cesare Montecucco

Dottoranda: Lucia Muraro

31 GENNAIO 2009

SUMMARY

RIASSUNTO 5
ABSTRACT 8
KEYWORS 11
Abbreviations 11
1 INTRODUCTION 12
1.1 Toxicity of BoNTs 12
1.2 The Diseases 12
1.2.1 Tetanus 12
1.2.2 Botulism 13
1.3 Structural Organization of Tetanus and Botulinum Neurotoxins 14
1.3.1 The Binding Domain 17
1.3.2 The Translocation Domain. 18
1.3.3 The Catalytic Domain 20
1.4 The Mode of Action of Clostridial Neurotoxins 21
1.4.1 Binding 22
1.4.2 Internalization 24
1.4.3 Membrane Translocation 26
1.4.4 SNARE Proteins' Specific Metalloproteolytic Activity 27
1.5 Clostridial Neurotoxins in Cell Biology 31
1.6 Therapeutic Uses 32
2 AIM OF THE THESIS 34
3 MATERIALS AND METHODS 35
3.1 Materials 35
3.2 Cloning Expression and Purification of N-terminal Half of the Binding Domain of Botulinum Neurotoxin Type A 35
3.3 Cell Cultures 37
3.4 Cell Imaging 37
3.5 Fluorescent Activated Cell Sorting (FACS) Analysis 38
3.6 Analysis of Membrane Fractions by Ultracentrifugation 39
3.7 Lipid Monolayer 40

3.8 Biochemical Assays and Blottings 42
4 RESULTS AND DISCUSSION 43
4.1 H_CN Portion of the Binding Domain Binds to Neuronal Cell Plasma Membrane 43
4.2 The H_CN Subdomains also Bind to Epithelial Cells but is not Sufficient for Transcytosis 47
4.3 Colocalization Analysis of EGFP-H_CN/A with Syntaxin and SV2A 49
4.4 The N-terminal Half of the Binding Domain of Botulinum Neurotoxin type A Binds to Sphingomyelin-containing Plasma Membrane Microdomains 51
4.5 EGFP-H_CN/A Localizes in Detergent-resistant Membrane Microdomains 54
4.6 Effect of Lipid Raft Perturbing Agents on EGFP-H_CN/A Binding to HeLa Cells 57
4.7 H_CN/A Interacts with Phospholipid Monolayers 61
4.8 The N-terminal Half of the Binding Domain of Botulinum Neurotoxin Type A Binds to Phosphatidylinositol Phosphate on Lipid Dot Blot 65
4.9 Bioinformatical Considerations 66
5 CONCLUSIONS 70
REFERENCEs 73

RIASSUNTO

Le neurotossine botuliniche (7 sierotipi di BoNTs, indicate con lettere dalla A alla G) e la tossina tetanica (TeNT) sono le più potenti tra le neurotossine clostridiali (CNTs), e sono responsabili rispettivamente del botulismo e del tetano. TeNT e BoNTs si legano ai terminali nervosi periferici e inibiscono il rilascio di neurotrasmettitori dalle cellule neuronali presinaptiche attraverso il taglio di proteine coinvolte nella fusione delle vescicole sinaptiche con la membrana cellulare. Le BoNTs agiscono a livello del Sistema Nervoso Periferico (SNP) causando paralisi flaccida, mentre TeNT agisce al livello del Sistema Nervoso Centrale (SNC) causando paralisi spastica. In particolare BoNT/A taglia la proteina associata ai sinaptosomi del peso di 25 kDa (SNAP25), bloccando il rilascio di acetilcolina alla giunzione neuromuscolare.

Dal punto di vista strutturale, le neurotossine clostridiali sono costituite da due catene polipeptidiche legate da un singolo ponte disolfuro: una catena denominata leggera (Light Chain, LC) di 50 kDa, che agisce nel citoplasma come una metalloproteasi; e una catena detta pesante di 100 kDa, che include un dominio di traslocazione (HN) e uno di legame al recettore (HC). Questi tre domini funzionali sono strutturalmente distinti e disposti in modo lineare senza contatto tra il dominio LC e quello HC. HC è a sua volta suddiviso in due sottodomini denominati H_CN e H_CC.

Queste neurotossine agiscono a concentrazione dell'ordine del femtomolare e il loro legame ad alta affinità è dovuto a siti di interazione multipli, sia a gangliosidi di membrana che a proteine specifiche della membrana neuronale. BoNT/A lega

le proteine delle vescicole sinaptiche, SV2 (Synaptic Vesicle 2) e al ganglioside GT1B. Data la suddivisione del dominio di legame era stato ipotizzato che i siti di legame si trovassero uno nel sottodominio H_CN e uno in quello H_CC. Il dominio H_CN ha una certa omologia di sequenza con le lectine, quindi sembrava un buon candidato per il legame ai gangliosidi. Recenti risultati cristallografici hanno mostrato che entrambi i siti di legame si trovano nel sottodominio H_CC. Vista la elevata omologia tra le tossine clostridiali è altamente probabile che anche il sito di legame al GT1B e alla proteina SV2 di BoNT/A si trovino sul medesimo sottodominio, il ruolo del dominio H_CN rimane quindi sconosciuto. Lo scopo di questo lavoro di tesi è di investigare il ruolo del sottodominio H_CN nel legame di BoNT/A alla membrana cellulare. È importante notare come la sequenza di questo sottodominio sia conservata tra le CNTs.

La sequenza di BoNT/A che codifica per H_CN (aa 855-1093) è stata clonata come proteina di fusione His-Tag, fusa con una proteina fluorescente verde (Enhanced Green Fluorescent Protein, EGFP) e con una rossa (monomeric cherry red fluorescent protein, mCherry). Con la tecnica della microscopia a fluorescenza abbiamo dimostrato che entrambe le chimere fluorescenti si legano alla membrana plasmatica di cellule epiteliali e neuronali. Il sottodominio fluorescente H_CN rimane legato alla membrana cellulare anche in seguito a incubazioni che permettono l'internalizzazione dell'intero dominio di legame H_C. La marcatura fluorescente non è omogenea, ma è concentrata in punti brillanti. Per la fase di legame di TeNT è già stato dimostrato un ruolo dei lipid rafts, ma il loro coinvolgimento non è così chiaro nel caso delle BoNTs. I nostri dati mostrano come la Lisenina, una tossina che lega in modo specifico la sfingomielina,

colocalizzi con la marcatura dovuta a H_CN, e che trattamenti con la sfingomielinasi diminuiscono il legame di H_CN alle cellule epiteliali. Inoltre con analisi di dot blot abbiamo dimostrato che H_CN è in grado di interagire lipidi anionici in particolar modo con il fosfatidilinositolo 5 fosfato (phosphatylinositol 5 phosphate, PI(5)P). Era già stato suggerito un ruolo dei lipidi carichi negativamente nel legame delle BoNTs e di TeNT al doppio strato lipidico, la nostra ipotesi è che la porzione N-terminale del dominio di legame sia in grado di legare il fosfatidilinositolo fosfato nel contesto dei lipid rafts. Noi suggeriamo che questa ulteriore interazione con la superficie cellulare possa svolgere un ruolo nel posizionamento della tossina per il suo successivo inserimento nella membrana.

ABSTRACT

Botulinum neurotoxins (7 serotypes of BoNTs, named from A to G) and tetanus neurotoxin (TeNT) are the most powerful clostridial toxins (CNTs). They are responsible for botulism and tetanus respectively. TeNT and BoNTs bind to peripheral nerve terminals and inhibit neurotransmitter release from presynaptic neuronal cells by proteolytic cleavage of proteins involved in the fusion of synaptic vesicles with the cell membrane. BoNTs act at the level of Peripheral Nervous System (PNS) causing flaccid paralysis whereas TeNT acts at the level of Central Nervous System (CNS) causing spastic paralysis. In particular BoNT A cleaves and disables SNAP25 (synaptosome-associated protein 25), impairing the release of acetylcholine at neuromuscular junction.

Structurally, CNTs are composed of two polypeptide chains linked by a single disulphide bond: the 50 kDa Light Chain (LC), which acts in the cytosol as a metalloprotease; and the 100 kDa Heavy chain, which includes a translocation domain (HN) and a receptor binding domain (HC). The three functional domains are structurally distinct and arranged in a linear fashion, such that there is no contact between the LC and HC domain. HC is further composed of two distinct subdomains H_CN and H_CC.

These neurotoxins act at femtomolar concentration and the high affinity binding is due to multiple binding sites, either for membrane ganglioside and neuronal specific membrane proteins. BoNT/A binds to SV2 (synaptic vesicle 2) and to the ganglioside GT1b. It was thought that these two binding sites were located one in H_CN subdomain and the other in the H_CC subdomain. H_CN share

some sequence homology with lectins so it was a good candidate to bind ganglioside. Recently by crystallographic analysis it has been shown that both the protein receptor and ganglioside sites of BoNT/B are in the H_CC domain. Due to the high homology between all CNTs it is likely that also the SV2 and GT1b sites are in the BoNT A H_CC domain. If this is the case the role of N-terminal subdomain of BoNT A is still unknown. The aim of this project is to investigate the role of H_CN in the binding of BoNT A to the plasma membrane. It is important to notice that the sequence of this toxin portion is conserved among all CNTs.

The sequence of BoNT/A coding for the H_CN domain (aa from 855 to 1093) has been cloned as His-Tag fusion protein, and fused to the Enhanced Green Fluorescent Protein (EGFP) and to the monomeric cherry red fluorescent protein (mCherry). By fluorescent microscopy observations we have shown that both the fluorescent chimera were able to bind to the plasma membrane of epithelial and neuronal cells. The fluorescent H_CN domain remains at the plasma membrane during incubation times that allow the internalization of whole binding domain, H_C. The fluorescent staining is not homogenous on the plasma membrane but is enriched in bright spots. For TeNT binding a role of lipid raft have been establish but for BoNTs the question seems to be still open. Ours data show that the sphingomyelin binding toxin lysenin, colocalized with H_CN staining and treatment with sphingomyelinase diminished the H_CN binding on epithelial cells. Moreover, in dot blot analysis H_CN was able to directly interact with anionic lipid in particular phosphatidylinositol 5 phosphate (PI(5)P). A role for negative charged lipid in the binding of BoNTs and TeNT to lipid bilayer, it was already suggested;

our hypothesis is that the N-terminal portion of the binding domain is able to bind anionic lipid in the environment of lipid raft. We suggest that these additional interactions with the membrane surface may play the role of positioning the toxin on the membrane surface ready for membrane insertion.

KEYWORS

Botulinum neurotoxin / botulism / sphingomyelin / PIP / membrane binding

ABBREVIATIONS

BSA, bovine serum albumin; BoNT, Botulinum neurotoxin; CL, Cardiolipin; ChOx, cholesterol Oxidase; DMEM, Dulbecco's Modified Eagle's Medium; DAG, Diacylglycerol; EBSS, Earle’s Balanced Salt Solution; EGFP, enhanced green fluorescent protein; FBS, foetal bovine serum; GM1, monosialoganglioside 1; H, heavy chain; HN, N-terminal portion of heavy chain; HC, C-terminal portion of heavy chain; H_CN, N-terminal portion of HC; H_CC, C-terminal portion of HC; L, light chain; SCMN, spinal cord motor neuron; MBCD, methyl-B-cyclodextrin; mCherry, monomeric red fluorescent protein; MEM, minimum essential media; NSC-34 neuroblastoma-spinal cord hybrid cell clone 34; PA, Phosphatidic Acid; PC Phosphatidylcholine; PFA, paraformaldehyde; PE, Phosphatidylethanolamine; PG, Phosphatidylglycerol; PI, Phosphatidylinositol; PI(3)P, PI(4)P, PI(5)P, PI monophosphates; PI(3,4)P, PI(3,5)P, PI(4,5)P, biphosphates; PI(3,4,5)P, PI triphosphate; S, Sulfatide (3-sulfogalactosylceramide); PS, Phosphatidylserine; SM, Sphingomyelin; SMase, sphingomyelinase, SNARE, soluble N-ethylmaleimide-sensitive fusion protein attachment protein receptor; SV, synaptic vesicle; SV2, synaptic vesicle protein 2; TG, Triglyceride.

1 INTRODUCTION

1.1 Toxicity of BoNTs

Synaptic transmission is a key process in nervous system physiology and synaptic vesicles are carriers of neurotransmitters signalling. Several pathogens had developed system to subvert host function at their advantage. An extraordinary example is the mechanism by which clostridial neurotoxins (CNTs) exploit synaptic vesicle recycling to enter the neuronal cells. In general neurotoxins block the transmission of nerve impulse by binding specifically to ion channels ensuing strong alteration of ion permeability and neurotransmission blockade. In contrast clostridial neurotoxins with their highly specific metalloproteolitic activity interfere directly with neurotransmitter release.

1.2 The Diseases

1.2.1 Tetanus

Tetanus may develop in different forms, and the most common one is the generalized tetanus caused by contamination of wounds or skin scratches with spores of toxigenic *Clostridium tetani*. Between the time of injury and the first symptoms there is a lag phase varying from few days up to four weeks. This time is necessary for (1) germination of spores, (2) toxin production and release, and (3) toxin diffusion, binding, transport to its target cells within the spinal cord. Tetanus usually begins with a characteristic lockjaw (risus sardonicus), with difficulty in swallowing and neck stiffness (Bleck, 1989). Afterward the muscle paralysis extends downwards to the muscles of the trunk, abdomen, and legs.

Later on, autonomic symptoms develop with alterations of blood pressure and of the cardiac rhythm and sweating possibly ending in cyanosis and asphyxia. Tetanus is often fatal, and death follows body exhaustion and usually intervenes by respiratory failure or heart failure. Following vaccination with tetanus toxoid (formaldehyde-treated tetanus toxin), tetanus has almost disappeared from the more developed countries, but it still takes hundreds of thousands of lives in those regions of the world where vaccination is not performed. Here, the major form of tetanus is tetanus neonatorum following the non sterile cut of the umbilical cord of babies born from non immunized mothers.

1.2.2 Botulism

Botulism causes less evident symptoms with a generalized muscular weakness causing diplopia, ptosis, dysphagia, facial paralysis, and reduced salivation and lacrimation. The paralysis then extend to the muscles of the trunk, including respiratory and visceral muscles. All the symptoms of botulism can be ascribed to the blockade of skeletal and autonomic peripheral cholinergic nerve terminals (Tacket, 1989). There are seven serotypically different BoNTs, labelled as BoNT/A trough BoNT/G. BoNTs are usually acquired via the oral route and the gravity of the illness depends on the amount and type of the toxins. BoNT/A, /B and /E account for most cases of human botulism, and the disease caused by BoNT/A is more dangerous with symptoms persisting much longer. The incidence and the types of botulism depend on the occurrence of toxigenic strains of *Clostridium botulinum*, *C. barati*, and *C. butyrricum* in the environment and subsequently in foods, and on the cooking practices. Home-prepared or –

stored/fermented food contaminated by spores of BoNT and conserved in anaerobic condition permit bacterial germination and are the cause of most of botulism outbreaks; contamination of foods prepared by food industries is very rare. Death comes up from the blockade of respiratory muscles, but if ventilated mechanically, the patient could recover completely. In general terms botulism is much less dangerous than tetanus because the amount of toxin that reaches the general circulation is not sufficient to block respiration.

A less common form of the disease is that of infant botulism, which follows the ingestion of spores of neurotoxigenic Clostridium that germinate and multiply within the intestinal tract. “Wound botulism” following spore contamination of wounds is very rare. On the contrary, animal botulism is rather common, and it can also be caused by BoNT/C and /D.

As a consequence of the fact that a single protein is responsible for all the clinical symptoms of tetanus and botulism, these diseases can be completely prevented by anti-toxin specific antibodies. Toxin neutralizing antibodies can be acquired passively by injection of immunoglobulins isolated from immunized donors or, actively, as a result of vaccination with toxoids, obtained by treating TeNT or BoNT with formaldehyde (Galazka and Gasse, 1995).

1.3 Structural Organization of Tetanus and Botulinum Neurotoxins

It is important to acknowledge that the structural organisation of these potent toxins has been the result of millions of years of evolution, during which time the relationship between structure and function has been developed to the extent that

the final product is considered to be the most potent natural toxin known to man. Despite the range of targets and the range of biological effects, CNTs have many common structural elements.

CNTs are synthesised as single-chain polypeptides of ~150 kDa and are subsequently cleaved to form di-chain molecules, in which the light (LC) and heavy chains are linked by a single disulphide bond. In fig 1 the di-chain structure of BoNT/A is shown (Turton et al., 2002).

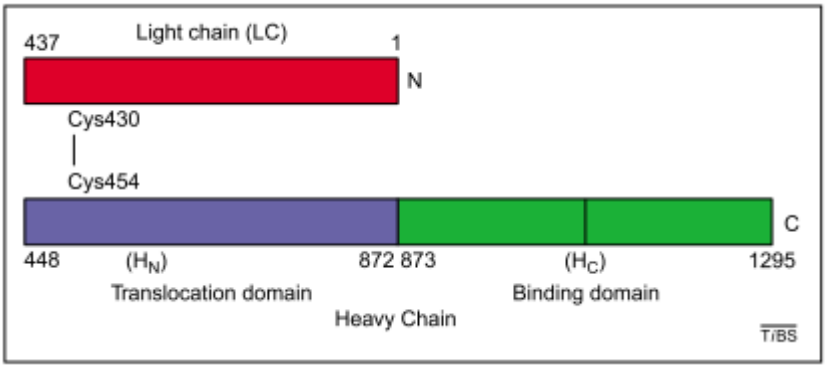

Figure 1 The di-chain structure of a Clostridial neurotoxin – Botulinum neurotoxin A (BoNT/A). Clostridial neurotoxins are ~150-kDa proteins, synthesized as single-chain polypeptides and post-translationally nicked to form di-chain molecules. They share the same domain architecture and overall structure. The light and heavy chains of BoNT/A are linked by a single disulfide bond, Cys430–Cys454. The light chain (LC), shown in red, functions as zinc-dependent endopeptidase and contains the catalytic zinc atom and HExxH motif associated with zinc-dependent proteases. The heavy chain comprises two functional domains of roughly equal size. The N-terminal section (HN), shown in blue, is the translocation domain, which forms ion channels spanning endosomal membranes and is thought to be involved in translocation and activation of the LC. The C-terminal section (HC), shown in green, is the binding domain. (Adapted from Turton *et. al*, TiBS 2002)

The 50-kDa LC acts as a zinc-dependent endopeptidase. The heavy chain contains two functional domains, each of ~50 kDa. The N-terminal half (H_N) is the translocation domain, known to form ion channels in lipid bilayers, and the C-terminal half (H_C) is the receptor binding domain, which has a key role in target cell membrane and subsequent internalization of the toxin molecules into

cholinergic neurons. The H_C binding domain consists of two subdomains, the N-terminal half (H_CN) and the C-terminal half (H_CC), each of 25 kDa. In terms of multi-domain organisation, CNTs are representative of the classical A-B type toxin structure, in which the holotoxin is the result of an association of two individual protein domains, each of which in itself is not toxic. The three functional CNT domains are structurally distinct and arranged in a linear fashion, such that there is no contact between the LC and HC domains.

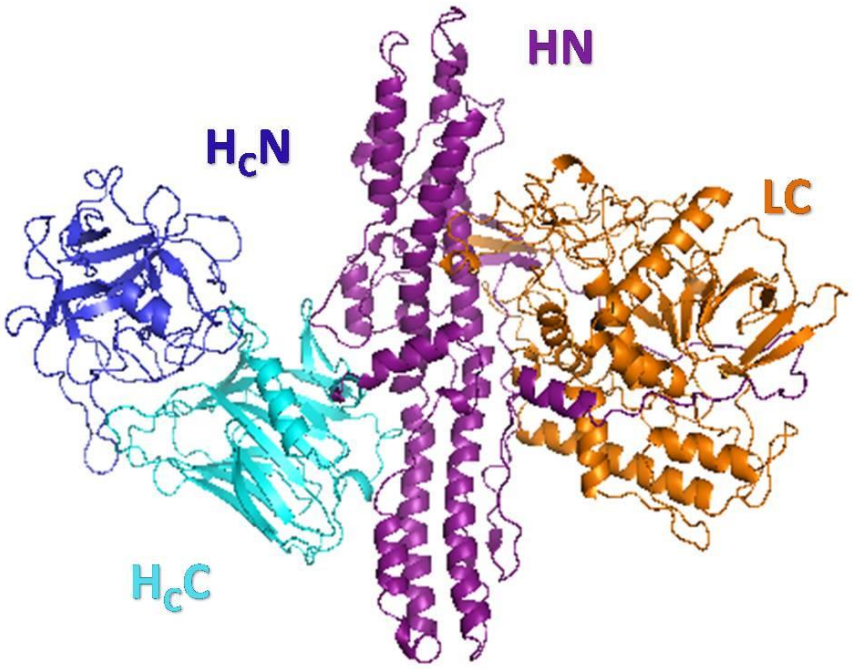

Figure 2 BoNT/A crystal structure. The three functional domains are each 50 kDa and correspond to the catalytic domain (LC. 1-437) in orange, the translocation domain (HN. 448-872) in purple and the receptor binding domain composed of, the N-terminal binding subdomain (H_CN. 873-1095) in light blue, and the C-terminal binding subdomain (H_CN. 1096-1295) in blue. This Figure was generated using PyMol DeLano Scientific.

In Fig. 2 the crystal structure BoNT/A is shown; this structure is highly conserved among CNTs as it is often the case with a protein family. Also the primary sequences are vastly conserved: overall, BoNTs and TeNT share ~35%

sequence identity (Lacy and Stevens, 1999); the BoNT catalytic LC domains share up to 36% sequence identity (Lacy and Stevens, 1999), and the LC domains of BoNT/B and TeNT have over 50% identity (Kurazono et al., 1992).

1.3.1 The Binding Domain

The HC binding domain of these CNTs consist of two distinct subdomains: the N-terminal half (H_CN) and the C-terminal half (H_CC), with little protein-protein contacts among them (Figure 2). The amino acid sequence of H_CN is highly conserved among CNTs; it is enriched in β-strands arranged in a jelly-roll motif closely similar to some carbohydrate binding proteins (legume lectins). The H_CC subdomain contains a modified β-trefoil folding motif present in several proteins involved in recognition and binding functions such as IL-1, fibroblast growth factor, and the Kunitz-type trypsin inhibitors. Its sequence is poorly conserved among CNTs. It harbours one binding site for the oligosaccharide portion of polysialogangliosides in BoNT/A and /B, while the H_CC of TeNT has two such sites (Rummel et al., 2003; Rummel et al., 2004b). H_CC of BoNT/B harbours also a cleft which fits in segment 44–60 of synaptotagmin belonging to the luminal domain of this SV protein (Chai et al., 2006; Jin et al., 2006; Rummel et al., 2007). The finding that for BoNT/B both binding sites are in the H_CC subdomain is in contrast with the previous idea that H_CC and H_CN contain each one a binding site. These neurotoxins act at femtomolar concentration and a double receptors model has been proposed to justify this extraordinary potency, early before structural details were discovered (Montecucco, 1986). In particular H_CN was thought to be the ganglioside binding domain, because of the similarity to lectin,

and H_CC to be appointed to protein receptor interaction. At the light of recent finding the role of the H_CN domain is still unknown.

1.3.2 The Translocation Domain

The N-terminal domain of the heavy chain is a fascinating polypeptide and is designed to deliver the LC from the endocytosed vesicle into the cytosol in order that the LC can access the SNARE substrate. HN has an elongated shape determined by a pair of unusually long and twisted α–helices, corresponding to segment 685-827 of BoNT/A (Lacy et al., 1998; Swaminathan and Eswaramoorthy, 2000). At both ends of the pair, there is a shorter α-helix which lies parallel to the main helices and, in addition, several strands pack along the two core helices. The overall structure of HN resembles that of some viral proteins undergoing an acid-driven conformational change (Bullough et al., 1994; Kielian and Rey, 2006; Weissenhorn et al., 1997). In addition to the paired α-helices, the HN domain also consists of an unstructured polypeptide that wraps around the LC to partially shield the active site channel (figure 2).

Two models of BoNT/B bound to both Syt-II and ganglioside have been generated with a different orientation of the translocation domain with respect to the cell membrane (Baldwin and Barbieri, 2007; Chai et al., 2006; Jin et al., 2006; Rossetto and Montecucco, 2007; Schiavo, 2006).

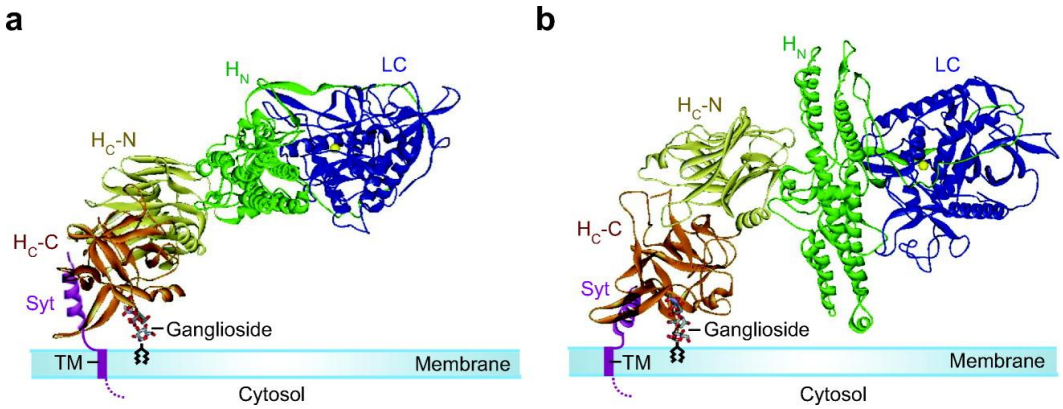

Figure 3 Binding of BoNT/B to the presynaptic neuronal membrane. Two different models have been proposed (Chai et al., 2006; Jin et al., 2006). The C-terminal part of the binding domain (H_CC in orange) binds both polysialogangliosides and the luminal domain of Syt-II (magenta). a) The helices of the translocation domain (HN) may be oriented in a parallel fashion (Chai et al., 2006) or b) sit orthogonal to the plane of the membrane surface (Jin et al., 2006). Proteins deposited in the Protein Data Bank under accession codes 1F31 (Swaminathan and Eswaramoorthy, 2000), 2NM1 (Jin et al., 2006), and 2NP0 (Chai et al., 2006) were used to model the complexes. The LC, the N terminal part of the heavy chain (HN), and the two C-terminal subdomains of the heavy chain (HC) are shown in blue, green, yellow, and orange, respectively. The yellow sphere represents the atom of zinc at the active site of the LC metalloprotease. TM =transmembrane domain.

Jin et al. (2006) suggest that the helices of the translocation domain sit orthogonal to the plane of the membrane (figure 3b). On the contrary, Chai et al. (2006) propose a parallel orientation, which would place hydrophobic areas of the helices close to the inner surface of the vesicle, facilitating their insertion into the membrane (figure 3a). The HN position with respect to the plasma membrane is a question of major interest because will give clue for the translocation step that is the less understood. It seems that HN domain is able to translocate a limited population of non-clostridial proteins across the endosomal membrane (Bade et al., 2004) and to function even in the absence of the HC domain (Chaddock et al., 2000). This data can be tested using the well developed and highly sensitive membrane translocation assay of BoNT/A developed by Montal and co-workers (Fischer and Montal, 2007).

1.3.3 The Catalytic Domain

The crystal structures of LC/A (Segelke et al., 2004), LC/B (Hanson and Stevens, 2000), LC/E (Agarwal et al., 2004), LC/D (Arndt et al., 2006), LC/F (Agarwal et al., 2005), LC/G (Arndt et al., 2005), and LC/TeNT (Breidenbach and Brunger, 2005) have been determined. They have a unique structure among metalloproteases. The active site zinc atom is coordinated by the imidazole rings of two histidines, a water molecule bound to the glutamic acid of the motif and a glutamic acid which is conserved among CNTs. The Glu residue of the motif is particularly important because it coordinates the water molecule directly implicated in the hydrolytic reaction of proteolysis. Its mutation leads to complete inactivation of these neurotoxins (Li et al., 2000). The active site is similar to that of thermolysin and identifies primary sphere of residues essential for catalysis, which coincides with the zinc coordinating residues. In addition, there is a secondary layer of residues, less close to the zinc centre, including Arg362 and Tyr365 (numbering of BoNT/A), which appears to be directly involved in the hydrolysis of the substrate (Binz et al., 2002; Rigoni et al., 2001; Rossetto et al., 2001a; Yamasaki et al., 1994). Structurally LCs are globular 50-kDa proteases with a mixture of both α-helix and β-strand secondary structure (figure 2). The active sites tend to be buried deep in the protein accessible by a channel, and full LC activity is only achieved following reduction of the single disulphide bond that covalently attaches the LC to the HN domain. The advent of LC structural information provided practical evidence of an array of substrate-binding sites remote from the active site (so-called exosites). In fact, rather than specific active site architecture, it is this multi-site binding approach that accounts for the

selectivity of the CNTs. This is the reason why enzymes with highly homologous active site regions, for example thermolysin, do not exhibit the ability to cleave SNARE proteins with any degree of specificity. In addition to tertiary sequence information, investigation of the LCs at the amino acid level has led to a suggestion of plasma membrane localisation and trafficking sequences being present at the N- and C-terminus of the protein, respectively (Fernandez-Salas et al., 2004).

1.4 The Mode of Action of Clostridial Neurotoxins

The structural organization of CNTs is functionally correlated with a four-step mechanism consisting of (1) binding, (2) internalization, (3) membrane translocation, and (4) enzymatic target modification (Montecucco et al., 1994; Montecucco and Schiavo, 1995; Rossetto et al., 2006). The carboxy-terminal part (HC) is mainly responsible for the neurospecific binding, the amino-terminal 50 kDa domain of the H chain (HN) is implicated in membrane translocation and, the LC is responsible for the intracellular catalytic activity. From the site of adsorption, BoNTs diffuse in the body fluids and eventually bind very specifically to the presynaptic membrane of cholinergic terminals causing flaccid paralysis. Normally BoNT/A are ingested and crosses intestinal cell monolayers via a receptor-mediated transcytosis mediated by the same neuronal protein receptor SV2 (Couesnon et al., 2008). At variance, the pathway of TeNT is more complex, as it involves an additional retroaxonal transport to the spinal cord and a specific binding to inhibitory interneurons, causing spastic paralysis (Lalli et al., 2003).

1.4.1 Binding

It was already introduced that both glycolipid and protein receptors are crucial for high-affinity binding to nerve cell membranes (Rummel et al., 2007). As BoNTs and TeNT are toxic at concentrations estimated to be < picomolar (Montecucco et al., 2004), binding has to be interpreted as the simultaneous occupation of the ganglioside binding pocket(s) and of the protein binding site. Polysialogangliosides are thought to be involved in BoNT binding as a result of the following observations: BoNTs bind to polysialogangliosides, particularly to GD1b, GT1b and GQ1b (Schiavo et al., 2000), and the HC fragments of BoNT/A and B bind to GT1b through the conserved peptide motif H…SXWY…G (Rummel et al., 2004b); pre-incubation of BoNTs with polysialogangliosides partly prevents the poisoning of the neuromuscular junction; pre-treatment of cultured cells with polysialogangliosides increases their sensitivity to BoNT/A, whereas depletion of gangliosides in neuroblastoma cells impairs BoNT/A internalization; treatment of membranes with neuraminidase, which removes sialic-acid residues, decreases BoNT binding; and knockout mice defective in the production of polysialogangliosides show reduced sensitivity to BoNT/A and BoNT/B (Bullens et al., 2002; Kitamura et al., 2005; Schiavo et al., 2000; Yowler et al., 2002). More recently, polysialogangliosides GD1b and GT1b and phosphatidylethanolamine were reported to be the functional receptors of BoNT/C and BoNT/D, respectively (Tsukamoto et al., 2005). However, polysialogangliosides alone do not account for the neurospecificity of binding of all BoNT serotypes. Indeed, SV proteins also participate in BoNT binding (table 1).

Table 1 Receptors for BoNT/A, BoNT/B and BoNT/G

Botulinum neurotoxin serotypes	Receptor	K_d/potency	Lipid requirement	Receptor expression at the neuro-muscular junction	Receptor expression in hippocampus/cortex excitatory neurons	Receptor expression in hippocampus/cortex inhibitory neurons
BoNT/B	Syt-I (Nishiki *et al*, 1996; Dong *et al*, 2003)	2.3 nM (Nishiki *et al*, 1996)	Yes (Nishiki *et al*, 1996; Dong *et al*, 2003)	No (Li *et al*, 1994; Marqueze *et al*, 1995)	Yes (Geppert *et al*, 1991)	Yes (Geppert *et al*, 1991)
BoNT/B	Syt-II (Nishiki *et al*, 1996; Dong *et al*, 2003)	0.23 nM (Nishiki *et al*, 1996)	Yes (Nishiki *et al*, 1996; Dong *et al*, 2003)	Yes (Li *et al*, 1994, Marqueze *et al*, 1995)	Yes (subpopulation; Geppert *et al*, 1991; Marqueze *et al*, 1995)	To be defined
BoNT/G	Syt-I (Rummel *et al*, 2004a)	Syt-I peptide 66% inhibition (Rummel *et al*, 2004a)	No (Rummel *et al*, 2004a)	See above	See above	See above
BoNT/G	Syt-II (Rummel *et al*, 2004a)	Syt-II peptide 37.9% inhibition (Rummel *et al*, 2004a)	No (Rummel *et al*, 2004a)	See above	See above	See above
BoNT/A	SV2C (Dong *et al*, 2006; Mahrhold *et al*, 2006)	Binding activity SV2C>SV2A>SV2B (Dong *et al*, 2006)	Yes, all isoforms (Dong *et al*, 2006)	Yes (Dong *et al*, 2006)	No Bajjalieh *et al*, 1994; Janz & Sudhof, 1999; Dong *et al*, 2006)	Yes (subpopulation only; C.V., C.G., M.M., unpublished data)
BoNT/A	SV2A (Dong *et al*, 2006)	Binding activity SV2C>SV2A>SV2B (Dong *et al*, 2006)	No (Mahrhold *et al*, 2006)	Yes (Dong *et al*, 2006)	Yes (Bajjalieh *et al*, 1994; Janz & Sudhof, 1999)	Yes (Bajjalieh *et al*, 1994; Janz & Sudhof, 1999)
BoNT/A	SV2B (Dong *et al*, 2006)	Binding activity SV2C>SV2A>SV2B (Dong *et al*, 2006)	No (Mahrhold *et al*, 2006)	Yes (Dong *et al*, 2006)	Yes (Bajjalieh *et al*, 1994; Janz & Sudhof, 1999)	No (Bajjalieh *et al*, 1994; Janz & Sudhof, 1999; C.V., C.G., M.M., unpublished data)

BoNT, Botulinum neurotoxin; K_d, dissociation constant; SV, synaptic vesicle protein; Syt-I and -II, synaptotagmin I and II.

BoNT/B and BoNT/G interact with the luminal domain of the SV proteins synaptotagmin I (Syt-I) and Syt-II. BoNT/B has a higher affinity for Syt-II (Nishiki et al., 1996), whereas BoNT/G interacts preferentially with Syt-I (Dong et al., 2003; Nishiki et al., 1996; Rummel et al., 2004a). The following experimental evidence suggests that this binding is physiologically relevant: Syt-II-transfected Chinese hamster ovary cells bind BoNT/B after treatment with polysialogangliosides (Nishiki et al., 1994; Nishiki et al., 1996) entry of BoNT/B (but not BoNT/A or BoNT/E) into PC12 cells is dependent on Syt-I and Syt-II (Dong et al., 2003); mice are partly protected from BoNT/B toxicity by fragments corresponding to the luminal domain of Syt-II (Dong et al., 2003); BoNT/B and BoNT/G interact with Syt-I and Syt-II in pull-down assays; and, finally, peptides derived from the Syt-I and Syt-II luminal domains are able to partly inhibit neurotoxicity at the phrenic neuromuscular junction (Rummel et al., 2004a). More recently, the specific interaction of BoNT/A with the luminal domain of SV2 has

been reported (Dong et al., 2006; Mahrhold et al., 2006). SV2 is highly glycosylated and has 12 putative transmembrane regions, similar to transporters with cytosol-exposed amino and carboxy termini (Bajjalieh et al., 1992). Tetanus toxin also shows multiple binding sites, two ganglioside binding sites (Rummel et al., 2003) and also to the GPI-anchored protein Thy-1 (Herreros et al., 2000).

1.4.2 Internalization

Several evidences indicate that CNTs do not enter the cell from the plasma membrane, but are endocytosed inside the lumen of vesicular structures. This process is temperature- and energy-dependent (Black and Dolly, 1986; Critchley et al., 1985; Dolly et al., 1984); reviewed in (Schiavo et al., 2000). The finding of SV proteins as receptors of BoNTs support the proposal (Montecucco and Schiavo, 1995) that, after binding, BoNTs are endocytosed within synaptic vesicles (SV) via their retrieval to be refilled with neurotransmitter (figure 4). This hypothesis was originally advanced to account for the increased rate of poisoning with NMJ activity (Hughes and Whaler, 1962). The different route of TeNT is probably due to the localization of its protein receptor in endocytic vesicles that moves in a retrograde direction along the axon.

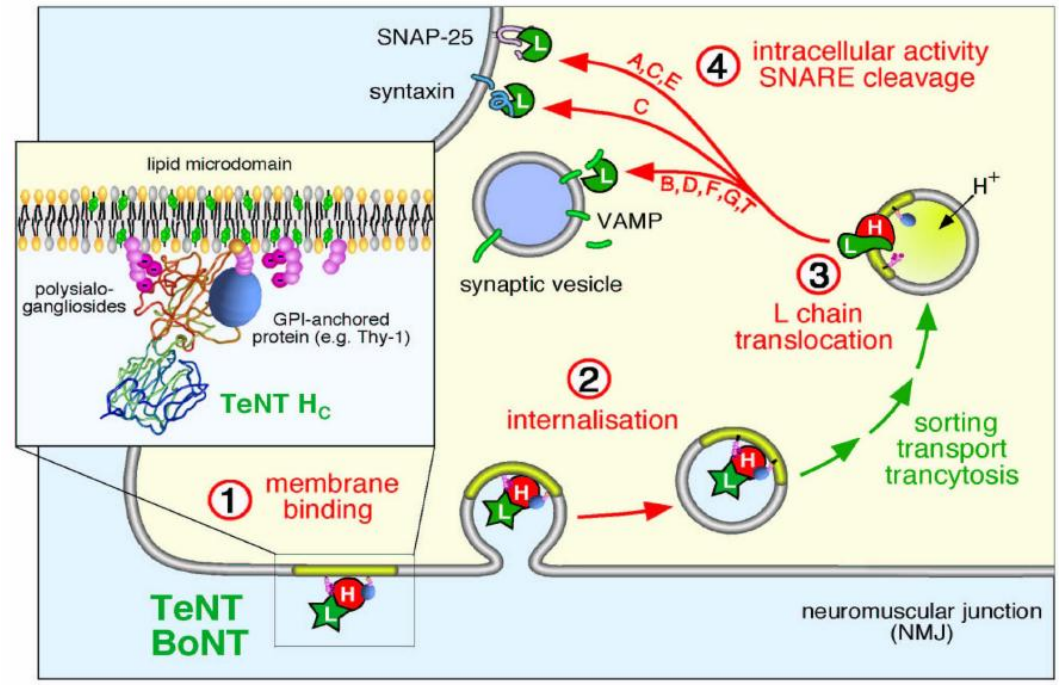

Figure 4 Binding and entry of CNTs at peripheral nerve terminal. (1) The BoNT binding domain associates with the presynaptic membrane of α-motoneurons through interaction with ganglioside and with the luminal domain of a synaptic vesicle protein upon SV membrane fusion. (2) BoNTs are endocytosed within synaptic vesicles via their retrieval to be refilled with neurotransmitter. TeNT exploits a pathway requiring lipid rafts and the clathrin machinery by binding to a lipid–protein receptor complex containing the ganglioside GD1b and a GPI-anchored protein Thy-1. Once internalized in clathrin-coated vesicles (CCV), TeNT is sorted into vesicle carriers of the axonal retrograde transport pathway. (3) At the low pH generated by the v-ATPase in the vesicle lumen, BoNTs change conformation, insert into the lipid bilayer of the vesicle membrane and translocate the L chain into the cytosol. (4) Inside the cytosol the L chain catalyses the proteolysis of one of the three SNARE proteins VAMP, SNAP-25 and syntaxin. The same four-step pathway of entry of BoNTs into peripheral nerve terminals is followed by TeNT in the inhibitory interneurons of the spinal cord, which are reached after retroaxonal transport.

TeNT-HC internalization at the motor nerve terminal occurs via a specialized clathrin-dependent pathway, which is distinct from SV endocytosis and is preceded by a lateral sorting from its lipid raft–associated ligand GD1b. (Deinhardt et al., 2006) (Roux et al., 2005). The TeNT-carrying vesicles reach the cell body of the motoneurons which reside within the spinal cord and then move to dendritic terminals to release the toxin in the intersynaptic space. TeNT then binds and enters the inhibitory interneurons of the spinal cord via SV endocytosis

(Matteoli et al., 1996). Consequently, it blocks the release of inhibitory neurotransmitters and impairs the system which controls the balanced movement of the skeleton, giving rise to a spastic paralysis. It is not known if, and if so, to what an extent, BoNTs migrate retroaxonally.

1.4.3 Membrane Translocation

The cellular targets of enzymatic activity of CNTs are in the cytosol, therefore at least the L chain must cross the hydrophobic barrier of the vesicle membrane. In order to do so, compelling evidence indicates that CNTs have to be exposed to low pH. (Matteoli et al., 1996; Simpson et al., 1994). In fact, acidic pH causes a conformational change from a water-soluble "neutral" structure to an "acid" structure with exposure of hydrophobic patches on the surface of both the H and L chains which then enter into the hydrocarbon core of the lipid bilayer (Montecucco et al., 1989; Puhar et al., 2004; Schiavo et al., 2000). Following this low pH-induced membrane insertion, BoNTs and TeNT form transmembrane ion channels in lipid bilayer (reviewed in Montecucco and Schiavo 1995) and in PC12 membranes (Sheridan 1998). The low pH-driven toxin conformational change takes place in a very narrow range of pH: 4.4–4.6 for TeNT and BoNT/A, /B, /C, /E, and /F (Puhar et al., 2004) and this similarity indicates that the key residues for the conformational change are conserved among CNTs and that they behave very similarly

with respect to lowering pH. Currently, membrane translocation is the least understood step of the mechanism of cell intoxication of CNTs, and further investigation is required to uncover the extent and implication of the structural

changes that occur at low pH. Koriazova and Montal (2003) have proposed that the H chain channel acts as a trans-membrane chaperone for the L chain, preventing its hydrophobicity-driven aggregation and maintaining its unfolded conformation during translocation. The L chain is then released into the neutral cytosol where it refolds into its native enzymatically active conformation. In this view, additional chaperones are not needed; however other bacterial toxins acting in the cytosol are assisted by complex of cytosolic chaperones and thioredoxin in their refolding (Haug et al., 2003; Ratts et al., 2003).

1.4.4 SNARE Proteins' Specific Metalloproteolytic Activity

The L chains of BoNTs and TeNT are highly specific proteases that recognize and cleave only three proteins of SNARE family, which form the core of the neuroexocytosis apparatus (Schiavo et al., 2000). TeNT, BoNT/B, /D, /F and /G cleave VAMP, a protein of the SV membrane, at different single peptide bonds; BoNT/C cleaves both syntaxin and SNAP-25, two proteins of the presynaptic membrane; BoNT/A and /E cleave SNAP-25 at different sites within the COOH-terminus (Humeau et al., 2000; Schiavo et al., 2000) (Figure 5). The molecular basis of the CNTs specificity for the three SNAREs resides on protein-protein interactions which extend well beyond the proteolysed SNARE regions, and a major role is played by a nine-residue-long motif present within the SNARE proteins. This motif is characterized by three carboxylate residues alternated with hydrophobic and hydrophilic residues (Breidenbach and Brunger, 2004) (Evans et al., 2005; Pellizzari et al., 1996; Rossetto et al., 1994) (Vaidyanathan et al., 1999; Washbourne et al., 1997). This motif is present in two copies in VAMP and

syntaxin and four copies in SNAP-25. The various CNTs differ with respect to the specific interaction with the recognition motif (Rossetto et al., 2001b). Only protein segments including at least one copy of the motif are cleaved by the toxins, and mutations within the motif inhibit the proteolysis (Fang et al., 2006); (Schiavo et al., 2000). Moreover antibodies against the SNARE motif inhibit the proteolytic activity of the neurotoxins (Pellizzari et al., 1997). A recent co-crystal structure of LC/A and SNAP25-(146–204) defined additional regions of interaction external to the cleavage site and to the motif (Breidenbach and Brunger, 2004; Breidenbach and Brunger, 2005). More recently, the fitting of an extended region of the substrate (residues 189–203) within the long active site cleft was defined following extensive mutagenesis of LC/A and SNAP-25 (Chen and Barbieri, 2006; Chen et al., 2007).

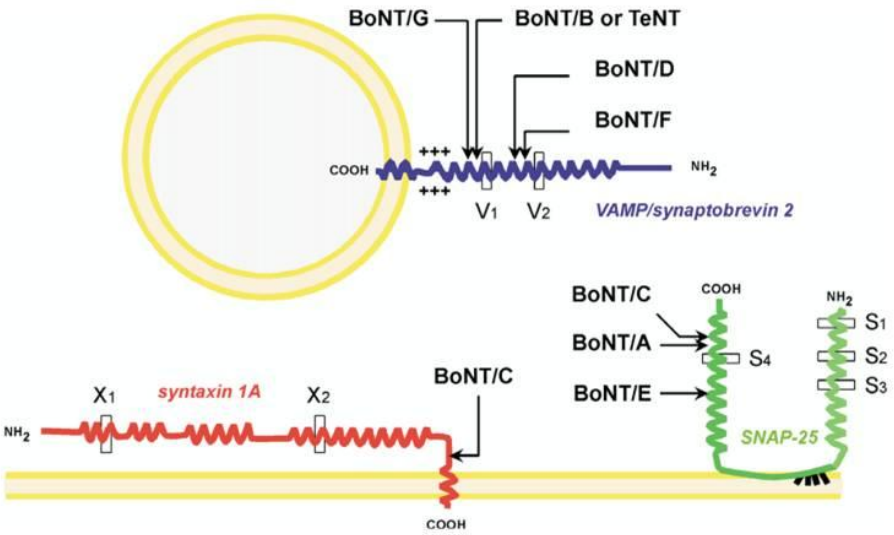

Figure 5 Molecular targets of clostridial neurotoxins. The three synaptic proteins cleaved by TeNT and BoNTs light chains are shown. The cleavage sites are indicated by arrows. The residues delimited by a box denote the sites that determine the binding specificity of the toxins light chains (also termed 'SNARE motif'). An additional binding site for the TeNT light chain on VAMP, rich in + charges, is indicated. (Adapted from Huemau et al. 2000)

BoNT-poisoned nerve terminals have a normal size and appearance with normal content and shape of synaptic vesicles and mitochondria (Duchen, 1971; Thesleff, 1960). VAMP, SNAP-25, and syntaxin form an heterotrimeric coiled-coil complex, termed the SNARE complex, which induces the juxtaposition of vesicle to the target membrane (Jahn et al., 2003; Sudhof, 2004). Several SNARE complexes assemble into a rosette in order to bring the SV membrane close enough to the cytosolic face of the presynaptic membrane to permit their fusion with subsequent release of the vesicle neurotransmitter content into the synaptic cleft (Montecucco and Molgo, 2005). Proteolysis of one SNARE protein prevents the formation of a functional SNARE complex and, consequently, the release of neurotransmitter. This is not true for BoNT/A and /C, which cleave SNAP-25 within few residues from the C-terminus giving rise to a truncated SNAP-25, which can still form a SNARE complex but not a rosette of SNARE complexes (figure 6).

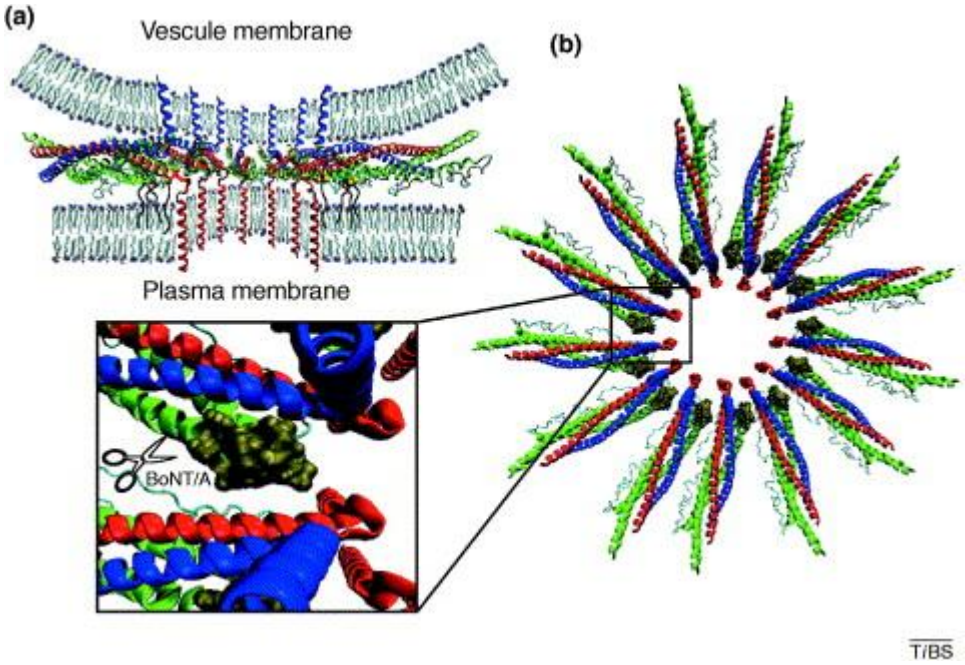

Figure 6. A model of the multimeric ring of SNARE complexes. The model is based on the X-ray structure of a complexin–SNARE complex (PDB code: 1KIL). (a) Side view of a cross section of SNARE super-complex. (b) Top view of the membrane fusion super-complex from the vesicle side.

Given the fact that a rosette of SNARE complexes is necessary for the exocytosis of one synaptic vesicle, the presence of a single defective SNARE complex will have a dominant negative effect on neurotransmitter release. This rationale explains the experimental finding that incomplete proteolysis of SNAP-25 at nerve terminals by BoNT/A is sufficient to cause full inhibition of neurotransmitter release (Bruns et al., 1997; Foran et al., 1996; Jurasinski et al., 2001; Keller et al., 2004; Osen-Sand et al., 1996; Raciborska et al., 1998; Williamson et al., 1996). This also explains the fact that the paralysis induced by BoNT/A and /C is long lasting, as the inhibitory activity of C-terminal truncated SNAP-25 on the assembly of the rosette of SNARE complexes overlaps and functionally extends the lifetime of the metalloproteolytic activity of the L chain of these two BoNTs (for a detailed discussion see Rossetto et al. 2006). These

explanations, however, may not be sufficient to account for the astonishing fact that the duration of the BoNT/A inhibition of autonomic nerve terminals is more than one year (Naumann and Jost, 2004). There are no quantitative data on the number of L chains required to intoxicate a nerve terminal. In Aplyisa californica cholinergic neurons, few molecules of toxin appear to be sufficient to block neuroexocytosis within an hour at room temperature (Poulain, personal communication). It is even more likely that few copies of L chain are sufficient in warm-blooded animals. It is evident that as long as the toxin is present in an active form, the nerve signal cannot be transmitted.

1.5 Clostridial Neurotoxins in Cell Biology

Pathogenic bacteria are able of rapid evolution and they have evolved sophisticated weapons to interfere with fundamental functions of higher eukaryotes. However, toxins are not only useful to the bacteria, they have also become an essential asset for life scientists, who can now use them as toolkits to explore cellular processes (for an extensive review see Schiavo and Van der Goot, 2001). Above other examples the receptor-binding unit of cholera toxin (CT-B) is a well establish tool to stain lipid raft enriched in the GM1 ganglioside, whereas the newly characterize Lysenin toxin binds to sphingomyelin (Yamaji et al., 1998).

First of all, due to their enzymatic activity botulinum and tetanus neurotoxins have been crucial in understanding membrane fusion, in particular during neurotransmitter release. The action of these toxins is restricted to neurons and neuronally differentiated cells, but cell permeabilization by means of pore-

forming toxins or transfection with the active domains of tetanus and botulinum neurotoxins allow the inactivation of specific SNAREs within any cell type. In addition, targeted expression of the active subunit of clostridial neurotoxins can be used to ablate specific SNARE proteins in selected tissues or even in entire organisms (Sweeney et al., 1995).

Secondly BoNT remain at the motoneurons synapse, allowing the study of site-specific endocytosis, whereas tetanus toxin is retrogradely transported to the cell body and then transcytosed to inhibitory interneurons, making it a marker of choice to study retrograde transport in neurons. In addition BoNTs can be used to follow transcytosis in binding-competent epithelial cells, using the toxin ability to enter the organism through the intestinal tract (Couesnon et al., 2008). A great advantage of CNTs is that the HC binding domain retain most of the binding and internalization proprieties, therefore fluorescent chimere of this domain can be used instead of whole toxins.

1.6 Therapeutic Uses

The demonstration that the inhibition of the nerve-muscle impulse is followed by a functional recovery of the NMJ provides the scientific basis of the rapidly growing use of BoNTs in the therapy of a variety of human diseases caused by hyperfunction of cholinergic terminals and other neurodiseases (Jankovic, 2006; Montecucco et al., 1996; Scott et al., 1989; Truong and Jost, 2006). Injections of minute amounts of BoNT into the muscle(s) to be paralyzed lead to a depression of the symptoms lasting months. Owing to the long lasting duration of its effect, BoNT/A has almost invariably been used (Figure 7).

Some human diseases treated with BoNT/A.

Disease/condition	Clinical effect	Benefit	Duration of effect (months)
Blepharospasm	Established	+++	2–4
Hemifacial spasm	Established	+++	2–6
Laryngeal dysphonia	Established	+++	1–6
Head and neck dystonias	Established	++	1–3
Strabismus	Established	++	Several months
Limbs dystonias	Established	++	1–3
Occupational cramps	Established	++	1–3
Anal fissures and rectal spasms	Established	+++	Several months
Palmar and ascellar hyperhydrosis	Established	+++	12
Hypersalivation and hypersweating	Established	+++	3–6
Migraine headache	Experimental	++	3–4
Pain	Experimental	+	Months
Bruxism	Experimental	+	2–6
Spasticity	Experimental	+	1–3
Urinary retention and pain	Experimental	++	1–2
Essential tremors	Experimental	+	1–3
Dysphagia and achalasia esophagea	Experimental	+/–	1–2

+++, very efficacious; ++, efficacious; +, low efficacy; +/– variable results in different studies.

Figure 7 List of various conditions that have been treated effectively with BoNT/A. (Montecucco and Molgo, 2005)

Since the NMJ paralysis is reversible, the injection has to be repeated, and the possibility of an immune response with production of BoNT/A-neutralizing antibodies can occur (Brin, 1997; Hanna et al., 1999; Jankovic and Schwartz, 1995; Sankhla et al., 1998; Zuber et al., 1993). The injection of a different BoNT serotype could overcome this drawback. BoNT/E and BoNT/F were tested in humans and were found to have beneficial effects of short duration (Aoki, 2001; Billante et al., 2002; Chen et al., 1998; Eleopra et al., 1998; Mezaki et al., 1995). Also BoNT/B has a rather short duration of action, and longer paralysis can only be achieved with very high doses, thus increasing the possibility of an immune response (Brin et al., 1999; Dressler and Bigalke, 2005; Dressler and Eleopra, 2006; Lew et al., 1997; Sloop et al., 1997). Studies performed in humans (reviewed in Eleopra et al. 2006) and in mice (Morbiato et al., 2007), show that BoNT/C has a general profile of action similar to that of BoNT/A.

2 AIM OF THE THESIS

Recent studies have led to the conclusion that the poorly conserved 25 kDa C-terminal half of the HC binding domain of BoNTs is the major responsible for their neurospecific binding and internalization inside SV. In order to justify the extraordinary potency of these toxins, early before structural details were discovered, a double receptor model was proposed (Montecucco, 1986). In particular H_CN was tough to be the ganglioside binding domain, because of the similarity to lectin, and H_CC to be appointed to protein receptor interaction. The finding that for BoNT/B both binding sites are in the H_CC subdomain opens the question on the role the 25 kDa N-terminal half of HC. The aim of this thesis is to investigate the role of this portion of this multi-component toxin. Due to his high sequence homology through BoNTs, it is likely that the H_CN sub-domain plays a common role within this toxin family.

3 MATERIALS AND METHODS

3.1 Materials

Escherichia coli XL1-Blue was from Stratagen; *E. coli* BL21 pLysS and anti His-tag antibody were from Novagen. pEGFP-N1 was from Clonetech. pRSETa, Alexa Fluor-555 goat anti-rabbit IgG, Alexa 488 goat anti-rabbit IgG antibody and SimplyBlue Safestain were from Invitrogen. Restriction enzymes were from New England Biolabs. HiTrap Chelating HP, ECL Advanced were from GE Healthcare Life Science. DMEM, MEM-EBSS were from Gibco; FBS was from Euroclone; Poly-$_{L}$-lysine, retinoic acid, gentamicin and optiprep, Cell Dissociation Solution Non-enzymatic (C 1419), propidium iodine, SMase, ChOX, MBCD, were from SIGMA. BSA, Complete Protease Inhibitor Cocktail and Expand High Fidelity PCR System were from Roche, Indianapolis, IN. Anti-GFP (Ab6556) was from Abcam; anti-flotillin was from BD Biosciences and anti-SNAP-25 clone SM181 from Sternberger. Monoclonal anti-VAMP-2 and anti-syntaxin were for Synaptic System. Membrane Lipid Strips and PIP array were from Echelon Biosciences.

3.2 Cloning Expression and Purification of N-terminal Half of the Binding Domain of Botulinum Neurotoxin Type A

The H_CN/A was cloned by PCR from pGEX-4T-3-Kin-HA-HCA (kind gift of Dr. G. Schiavo, Cancer Research UK). Forward and reverse primer sequences were 5'-AAACTCGAGAGTACAGATATACCTTTTCAGCTT and 5'-AAAAAGCTTTGAATTTGATTGATTATCATATAAATCTTT respectively.

The DNA fragments obtained were digested with *Xho*I and *HindIII*, introduced at overhangs of the used oligonucleotides, and inserted into the vector pRSETa . The EGFP sequence was cloned from pEGFP-N1 and mCherry was cloned from pRSETb-mCherry (Shaner et al., 2004). Forward and reverse primer sequences were 5' AAAGGATCCATGGTGAGCAAGGGCGAG 5'-AAACTCGAGCTTGTACAGCTCGTCCATGCC, for both EGFP and mCherry sequences. The amplified sequences were digested with *BamHI* and *XhoI* and H_CN/A sequence was cloned in the pRSETa, pRSETa-EGFP and pRSETa-mCherry vector to obtain pRSETa- H_CN/A, pRSETa-EGFP-H_CN/A or pRSETa-mCherry-H_CN/A. DNA inserts sequencing were sequenced by CRIBI (Padua).

BL21 (DE3) pLysS *E. coli* strain transformed either with pRSETa- H_CN/A, pRSETa-EGFP-H_CN/A or pRSETa-mCherry-H_CN/A were grown in LB medium until the OD_{600} (optical density at 600 nm) reached 0.6. Cultures were induced with 1 mM IPTG (isopropyl β-D-1-thiogalactopyranoside) for 4 h at 30°C. Cells were pellet, frozen in liquid nitrogen and keep at -80°C. Cells were then lysed by two passages of pre-cooled French Press. The lysate was centrifuged (17,000 x g, 20 min), and the supernatant was loaded on a HiTrap Chelating HP on a ÄKTAprime system (GE Healthcare) and eluted with a linear gradient from 0 to 500 mM Imidazole. Protein purity was assessed by staining with SimplyBlue Safestain of a 12% SDS–PAGE gel. Protein identity was confirmed by Western blotting using an anti-His-Tag antibody. pRSETa-EGFP-HC/A were described in Laura Morbiato PhD thesis, March 2006.

3.3 Cell Cultures

Primary rat spinal *cord* motor neurons (SCMNs) were isolated from Sprague-Dawley rat embryos (embryonic day 14) and cultured following previously described protocols (Bohnert and Schiavo, 2005). All experiments were performed using SCMNs differentiated for 5–8 d. NSC-34 is an immortalized motor neuron cell line, (kindly provided by Dr A. Poletti, University of Milan, Italy). These cells were routinely maintained in DMEM with sodium pyruvate, supplemented with 10% FBS, 100 UI/mL of gentamicin and grown at 37°C in 5% CO_2 in 25 cm^2 flasks, changing medium every 72 h. Cells were induced to differentiate in DMEM 5% FBS containing 10 μM retinoic acid. For live-imaging and immunofluorescence, cells were seeded on glass-bottomed Petri dishes (Matek) previously coated with poly-L-lysine. For biochemical analysis and detergent-resistant microdomains isolation, cells were seeded on 60 mm Petri dishes. NSC-34 cells were used at the 5^{th} day of differentiation. HeLa cells were cultivated in MEM-EBSS supplemented with 10% FBS, Caco-2 cells in MEM-EBSS, 15% FBS and 1% non essential amino acids and detached with 0.05% trypsin when confluent. T84 cells were grown in DMEM, Ham's F-12 Medium 1:1, 15 mM hepes, 10% FBS and detached with 0.25% trypsin when confluent.

3.4 Cell Imaging

SCMNs or differentiated NSC-34 were incubated with 200 nM or 50 nM EGFP-H_CN/A respectively, in E4 buffer supplemented with 0.5 %BSA for 30 minutes at 37°C. HeLA and Caco-2 were incubated 200 nM EGFP-H_CN/A in MEM-EBSS medium supplemented with 0.5% BSA 30 minutes at 37°C.

mCherry-H_CN/A was used 250 nM on NSC-34 cells and 1 μM on HeLA or Caco-2 cell. Venus-NT-Lysenin was used 100 nM on NSC-34, HeLA and Caco-2 cells. After washing, cells were observed under the fluorescence microscope. NSC-34 cells were fixed with 4% PFA followed by quenching with NH_4Cl, whereas HeLa and Caco-2 cells with cold acetone. The samples were then washed with PBS containing 2% BSA and 0.2% gelatin for NSC-34 and SCMNs, and PBS 2% BSA for HeLA and Caco-2 cells. Plasma membrane-localized EGFP-H_CN/A was stained with a rabbit antibody specific for the GFP used at 1:10'000 dilution, followed by an Alexa Fluor 555 goat anti-rabbit IgG antibody (Invitrogen). The previously surface-stained cells were permeabilized with 0.1% Triton X-100 for 3 min at room temperature, and after a second blocking step, a second labelling of the chimeric protein was carried out with the same rabbit antibody and an Alexa Fluor 488 goat anti-rabbit IgG antibody (Invitrogen) was used as secondary antibody.

Fluorescence images were acquired with a Leica AD MIRE3 inverted microscope, equipped with a Leica DC500 CCD camera, x63 oil immersion objective and x1.5 zoom (NA 1.4). Stacks were acquired along the z-axis with 0.27 μM spacing. Data were collected using the Leica FW4000 software and analyzed with Leica Deblur and WCIF ImageJ; stacks were de-convoluted and a single 3D cell image was obtained.

3.5 Fluorescent Activated Cell Sorting (FACS) Analysis

HeLA cells were seeded 40'000 cells/well in 24 well plates and used 2 days after. The day of the experiment the cells were washed three times in PBS 0.5%

BSA and incubated with EGFP-H_CN or Venus-NT-Lysenin for 30 min in the same buffer at 37 °C or 4°C. When necessary preincubation with lipid rafts perturbing agents was performed prior the addition of EGFP-H_CN or Venus-NT-Lysenin. We performed preliminary screening of concentrations and protocols for each chemical, and the cytotoxicity of treatment have been controlled with propidium iodine. Propidium Iodine is a fluorescent DNA dye that could enter only dead cells. We decide to use: Cholesterol Oxidase (ChOx) 1u/ml 2h; sphingomyelinase (SMase) 0,5 u/ml 1h; methyl-B-cyclodextrin 2.5 mM 1h. For studying the resistance of the binding of EGFP-H_CN to detergent, cells have been incubated for 30 min at 4°C with 1% Triton X-100 after EGFP-H_CN/A incubation.

After the treatment cells were detached with Non-enzymatic Cell Dissociation Solution (SIGMA c5914) and transferred in a 96 well round bottom plate, put on ice and washed three times with cold FACS buffer (PBS 1 % FBS). Propidium iodide was added to exclude dead cells, and cell fluorescence intensities of the gated populations were measured with a FACS Calibur flow cytometer equipped with CellQuest software (Becton Dickinson, San Jose, CA, USA) further analysis have been performed with WinMDI version 2.9 (Scripps Research Institute).

3.6 Analysis of Membrane Fractions by Ultracentrifugation

Five-days differentiated NSC-34 cells were grown on 6 cm culture dishes, rinsed with E4 buffer (Hepes 10 mM 7.4, 120 mM NaCl, 3 mM KCl, 2mM $CaCl_2$, 1,2 mM $MgCl_2$, and Glucose 10mM) and then lysed on ice with 375 µl of precooled TXNE buffer (50 mM Tris–HCl, 150 mM NaCl, 5 mM EDTA, pH 7.4, 0.1% Triton X-100), additionated of Complete Protease Inhibitor Cocktail. Cells

were homogenized by passing for three times the ice-cold lysates through a 22G needle. Extracts were adjusted to 35% OptiPrep , placed in a SW40Ti ultracentrifuge tube (Beckman, Palo Alto, CA), and over-layed with 8.75 ml of 30% OptiPrep in TXNE and then with 1 ml of TXNE. After centrifugation (4 hr, 200,000 x g, 4°C), ten fractions were collected from the top, and analyzed by Western blotting using antibodies specific for GFP antibody, for flotillin-1 and for SNAP-25.

3.7 Lipid Monolayer

In this technique a lipid mixture, usually dissolved in chloroform, is dispersed on an aqueous solution, leading the formation of an oriented lipid monolayer with polar head of the phospholipids facing the solution (figure 8).

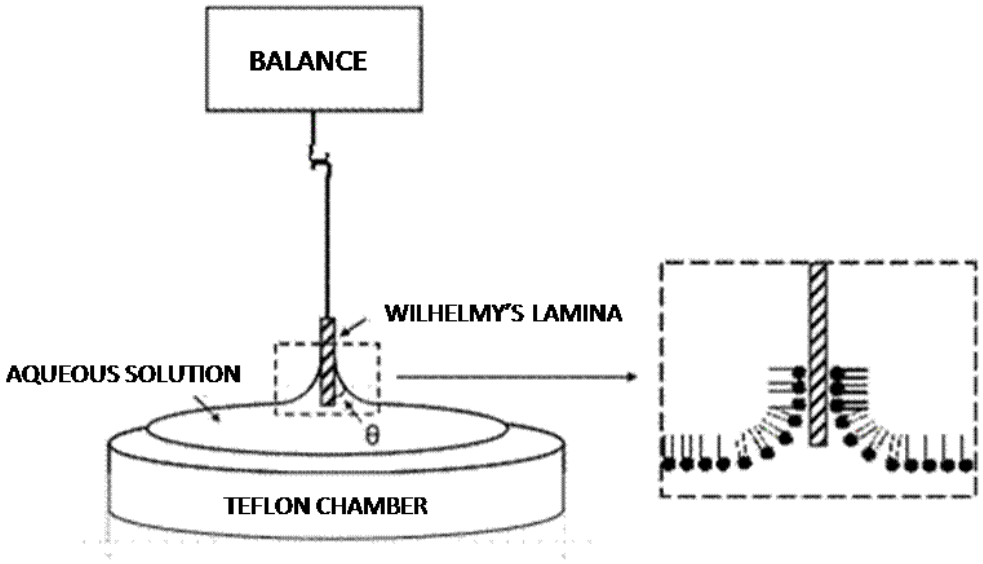

Figure 8 Schematic representation of the Wilhelmy balance. The lamina is partially immersed in an aqueous solution overlaid by a lipid monolayer (broken line area inset). The lamina is connected to the balance for registration of surface pressure variation.

Using lipid monolayer to study protein-lipid interaction has several advantages; the model system is very stable; the geometry of lipid is planar with a know orientation. Thus the lipid monolayer system is a good model to study protein-lipid interaction in condition similar of those of an approaching protein to cellular membrane from the extracellular medium (Maget-Dana, 1999). The system is composed of a platinum lamina partially immersed in the solution and connected to an electron-microbalance to register the variation of surface pressure.

When a protein is injected in the solution and it inserts in the membrane the electron-microbalance register an increase of surface pressure. Following the kinetic profile is possible to distinguish an initial phase of insertion that reaches finally a saturation point (figure 9).

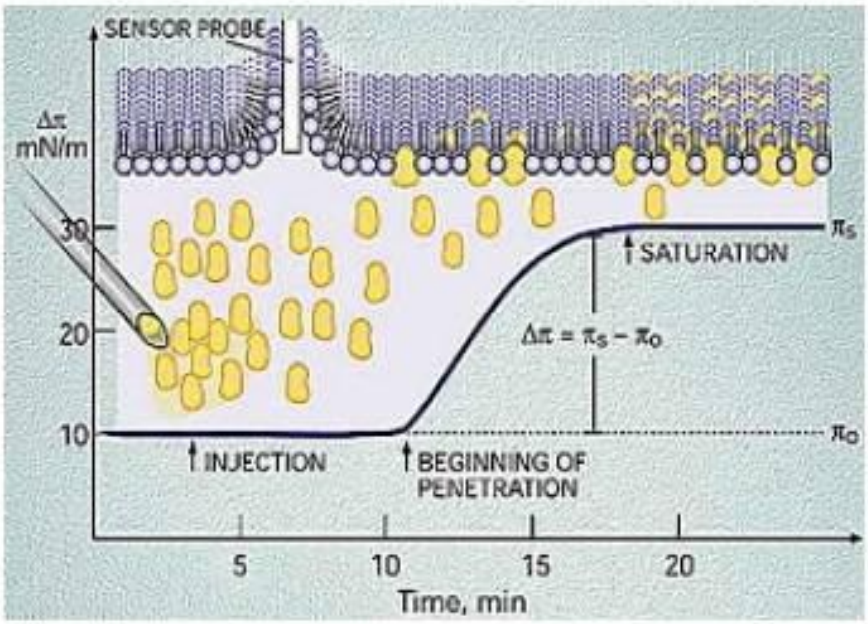

Figure 9 Schematic representation of the insertion of a protein in a lipid monolayer. The protein is injected in the aqueous solution below the lipid monolayer, and its insertion in the membrane increases the surface pressure until a saturation point.

We used a Delta Pi (Kibron) instrument connect with a Delta Graph software equipped computer, that permit to follow the kinetic of surface pressure variation. The set-up allow to use very small volume of buffer using a 600 µl chamber and a thinner (∅ 0.51 mm) probe instead of the lamina, however the sensitivity is very high (10µN/m). Several lipid composition stocks have been prepared at the concentration of 0.1 or 0.025 mg/ml. Small drop of lipid are added at the air-buffer interface with a micropipet, it is important that the drop are small to allow the solvent evaporation and avoid lipid dispersion in the medium. Normally few µl of lipid stock are sufficient to get the desiderate surface pressure of 22 mN/m. The surface pressure of a cellular membrane has been estimated in 30 mN/m, but 22 mN/m is the initial pressure value normally used in the specialized literature. We used a buffer 10 mM sodium phosphate, 10 mM sodium citrate, 125 mM sodium chloride and 0.5 mM EDTA at pH 7.4, we added 9.6 µl of orthophosphoric acid 8.5% in 600 µl chamber to acidify the pH to 5. Between the different measures the chamber is washed several times with water and organic solvent and platinum probe is burned to eliminate any residues of the previous experiment.

3.8 Biochemical Assays and Blottings

EGFP-H_CN/A bound to NSC34 cells was estimated on 24-wells plates seeded with 6000 cells/well and incubated with the chimeric protein under the conditions described above. Cells were mechanically resuspended and dissolved in a lysis buffer (Promega). These samples and the gradient fractions were solubilised in Laemmli SDS buffer, boiled and loaded onto 10% or 12% polyacrylamide gels.

After electrophoresis, the samples were transferred on nitrocellulose sheets, probed with a rabbit anti-GFP antibody 1:10’000, and stained with a goat anti-rabbit IgG coupled to horseradish peroxidase and developed with ECL Plus.

Membrane Lipid Strips and PIP arrays were used according to manufacture instructions (Echelon Bioscience), incubated with 0.015 µg/ml of EGFP-H_CN/A, and revealed with anti-GFP antibody 1:10’000, goat anti-rabbit IgG horseradish peroxidase followed by ECL Plus.

4 RESULTS AND DISCUSSION

4.1 H_CN Portion of the Binding Domain Binds to Neuronal Cell Plasma Membrane

To study the role of H_CN subdomain and in particular its capacity of membrane interaction, we expressed and purified the recombinant H_CN subdomain of BoNT/A, abbreviated as H_CN/A, and the protein chimera with enhanced green fluorescent protein (EGFP), abbreviated here as EGFP-H_CN/A and to mCherry red fluorescent protein, abbreviated as mCherry-H_CN/A. For the EGFP-H_CN/A we controlled that the folding of the H_CN subdomain is conserved. We performed far-UV circular dichroism of EGFP-H_CN/A and EGFP protein alone and we mathematically subtracted the EGFP contribution. We obtained that the overall secondary structure composition was the same of deposited crystallographic structure (PDB code 3BTA) (not shown).

We first of all decide to incubate EGFP-H_CN/A with the target neuronal cells, and to use experimental conditions that normally allow HC internalization. We

decide to use SCMNs and differentiated NSC-34 cells as models; cells were then incubated with the fluorescent chimeras for 30 min at 37°C. Figure 10 shows a staining of the plasma membrane on spinal cord motoneurons and NSC-34 cell line on live imaging, the staining is not homogeneous on the cellular surface but it is concentrated in discrete spots. The EGFP variant is pH sensitive and it is quenched at acidic pH, but even when cells were observed after one hour from the incubation end point there is no evidence of quenching (not shown). This gives the first clue that H_CN is sufficient for the binding but is not able to trigger the internalization step.

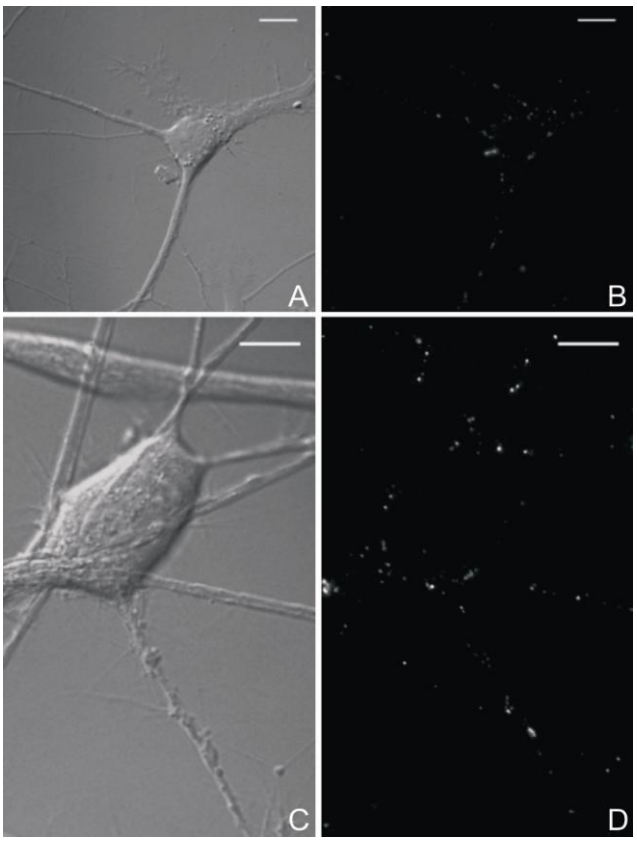

Figure 10 Binding of EGFP-H_CN/A to primary spinal cord motoneurons and NSC-34. Live imaging of spinal cord motoneurons (A,B) and differentiated NSC-34 (C,D) incubated at 37°C for 30 min with 200 nM or 50 nM EGFP-H_CN/A respectively. Scale bars: 10 μm. EGFP alone does not bind to these cells and GFP Western blot analysis of the EGFP-H_CN/A treated cells did not show any band corresponding to EGFP protein alone (not shown).

To confirm this initial hypothesis we performed an indirect immunofluorescence against EGFP to allow the visualization of quenched (internalized) chimera. In particular we used a protocol that discriminate plasma membrane bound protein from intracellular protein. Briefly two different EGFP staining were performed with two different secondary antibodies, interposed by cell permeabilization. Several stacks have been acquired along the Z-axis, and superimposed to create a unique projection. In figure 11 an almost complete colocalization of the staining is shown, meaning that the whole EGFP-H_CN/A staining is due to plasma membrane bound protein.

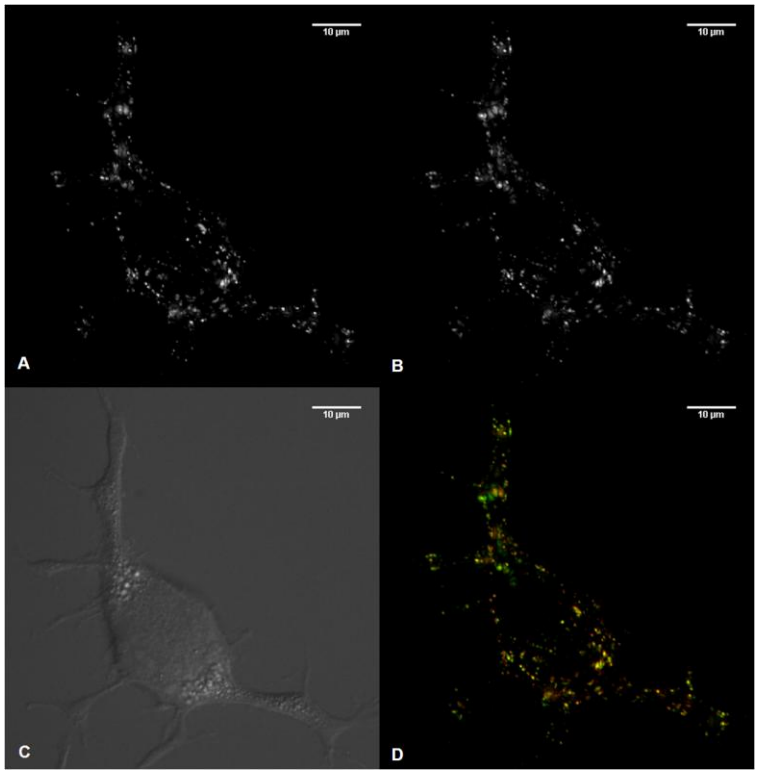

Figure 11 Immunofluorescence staining of EGFP-H_CN/A before of after permeabilization. Plasma membrane-localized EGFP-H_CN/A was stained with a rabbit antibody specific for the GFP used at 1:10'000 dilution, followed by an Alexa Fluor 555 goat anti-rabbit IgG antibody (A). The previously surface-stained cells were then permeabilized with 0.1% Triton X-100, for 3 min at room temperature. After a second blocking step, the labelling was carried out with the same rabbit antibody and an Alexa Fluor 488 goat anti-rabbit IgG antibody (B) was used as secondary antibody. The corresponding bright field (C) and merged imaged (D) are also shown.

Furthermore, if we analyze the stacks sequence of the staining performed after the permeabilization is evident that the staining follows the plasma membrane profile and that there is no intracellular signal (Figure 12).

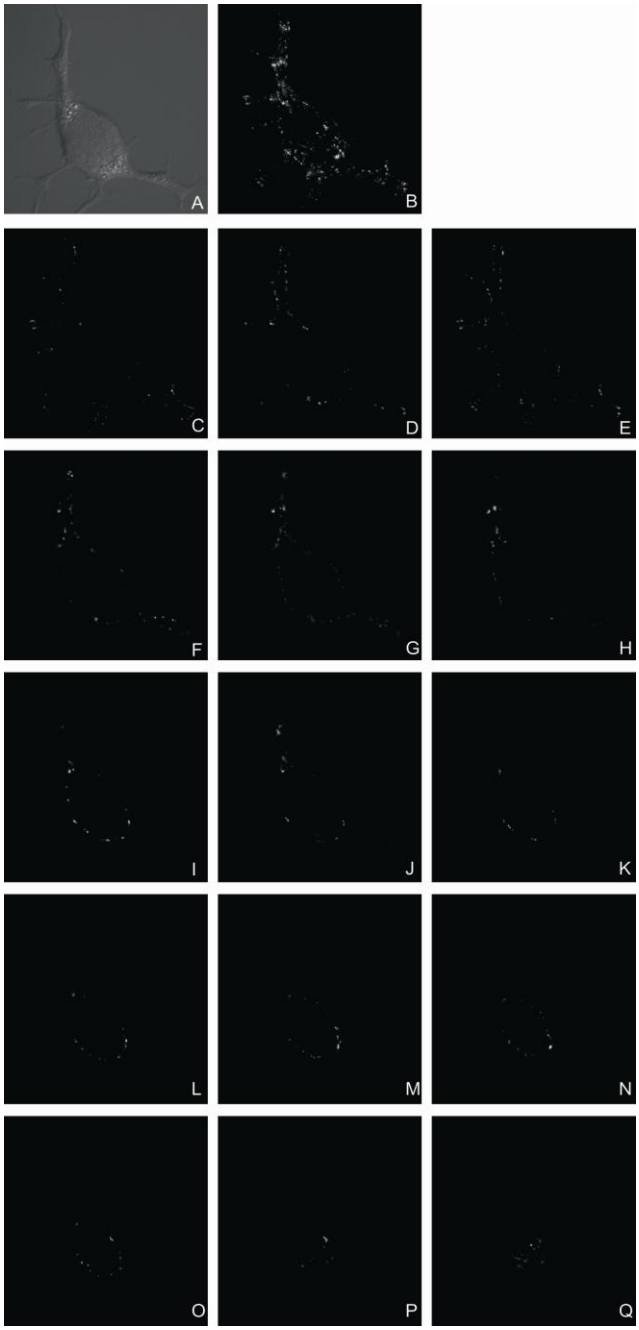

Figure 12. Immunolabelling of EGFP-H_CN/A after permeabilization. This figure shows all the stacks (C-Q) acquired along the Z-axis in the green channel, the 3D reconstructed image (B) and the corresponding bright field (A).

The conclusion that H_CN/A is able to bind to cells, and that such binding is not sufficient to trigger internalization is suggested by the following data: a) the surface distribution was never followed by internalization, as indicated by its morphology (figure 12); b) any fluorescence quenching, which would follow exposure of the EGFP moiety to the acidic pH of the endosomal lumen; was never observed; c) the staining of EGFP-H_CN/A revealed with an anti-GFP antibody with or without membrane permeabilization was coincident (figure 11). Furthermore, no intracellular staining was ever observed when the pH insensitive mCherry-H_CN was used (not shown).

4.2 The H_CN Subdomains also Bind to Epithelial Cells but is not Sufficient for Transcytosis

In order to test if EGFP-H_CN/A binding is neurospecific,two epithelial cell lines were also investigated: HeLa cells deriving from an ovary cancer and CaCo-2 cells deriving from a colorectal adenocarcinoma. The latter are more physiologically relevant because BoNTs enter the body through gut, and CaCo-2, upon reaching confluence, express characteristics of enterocytic differentiation. Surprisingly, the EGFP-H_CN/A chimera exhibited the same discrete and spotty binding we observed in neuronal cells (Figure 13).

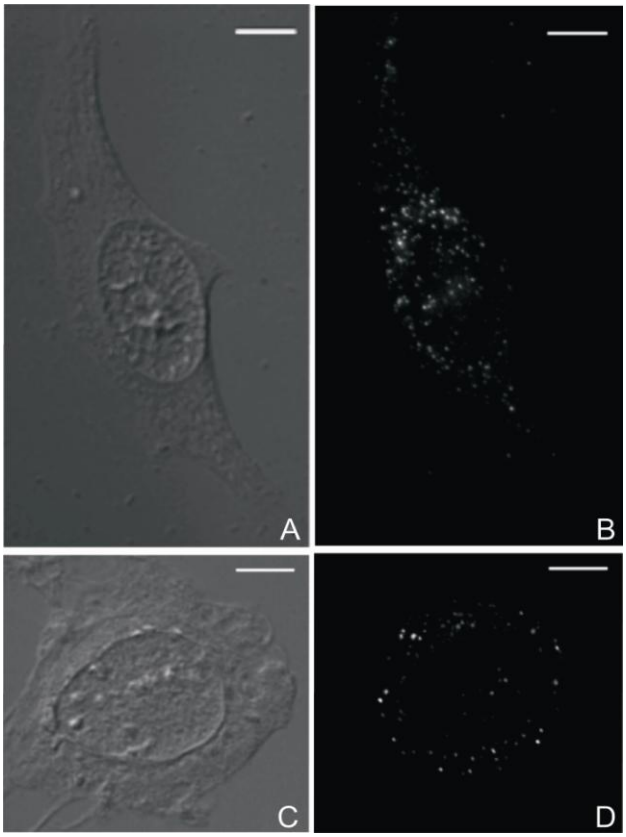

Figure 13 Binding of EGFP-H_CN/A to HeLa and Caco-2 cell lines. HeLa cells (A,B) and Caco-2 (C,D) were incubated at 37°C for 30 min with 200 nM EGFP-H_CN/A, and fixed with cold acetone. Several stacks have been acquired along the Z-axis and the fluorescence images are the result of their superimposition. Scale bars: 10 μm. EGFP alone does not bind to these cells (not shown).

It has been shown that the whole HC domain is sufficient to be transcytosed from apical to basolateral side of polarized monolayer of gut epithelial cell lines (Couesnon et al., 2008). Due to the ability of H_CN/A to bind epithelial cell we decide to investigate if this subdomain could be sufficient for transcytosis. We used T84 cell line derived from a lung metastasis of a colon carcinoma in the same experimental condition of Couesnon et al. 2008. The whole binding domain fused to EGFP, EGFP-HC/A, was able to cross the polarized monolayer, as expected, whilst EGFP-H_CN was not (figure 14).

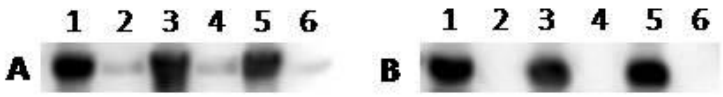

Figure 14. H_CN domain is not sufficient for transcytosis in polarized epithelial cells monolayer. T84 cells have been seeded on a transwell chamber and let differentiate for 15 days. The integrity of monolayer was checked using transepithelial electrical resistance (TER). EGFP-HC/A (panel A) or EGFP-HCN/A (panel B) was added to upper part of the transwell chambers. After 18 h incubation SDS-page samples were prepared from the medium of upper and lower part of three transwell chambers and anti-GFP western blot analysis was performed. EGFP-HC/A is found in triplicate (lane 2, 4, 6 panel A) in the lower side of the transwell chamber meaning that it has been transcytosed. The major portion of the fluorescent chimera is still in the upper part (lane 1, 3, 5), meaning that the process is not very efficient. On the contrary EGFP-H_CN/A is only found in the upper side (lane 1, 3, 5 panel B), meaning that it has not been transcytosed.

From this second line of evidences we cannot exclude that H_CN is involved in transcytosis but it is not sufficient for the trigger this intoxication step. We can conclude that this toxin portion has a general cell binding activity and that this ability could contribute to justify the enormous potency of this toxin family.

4.3 Colocalization Analysis of EGFP-H_CN/A with Syntaxin and SV2A

Since it is well demonstrated that BoNTs exploits synaptic vesicles recycling to enter the cells, we then decide to investigate if there could be any relationship between the H_CN spotty staining and the synaptic activity: at the synapse SNARE proteins are enriched and the characteristics of EGFP-H_CN/A staining could be due to the interaction with one of this protein. We chose an immunofluorescence approach to compare distribution of EGFP-H_CN/A on the membrane and proteins involved in synaptic function. We performed colocalization experiments with several of these proteins but there is no evident colocalization between EGFP-

H_CN/A and anyone of them. In figure 15 are shown the results relative to syntaxin and in figure 16 those relative to a protein mainly enriched in SV, synaptic vesicle protein 2 (SV2).

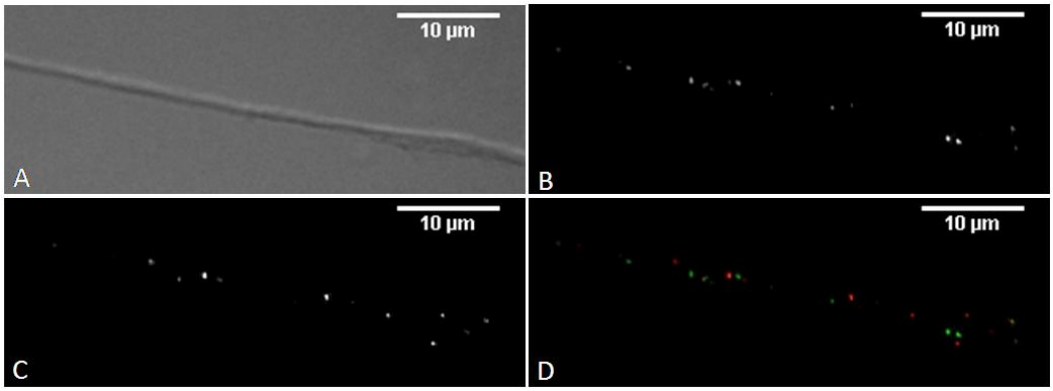

Figure 15 Colocalization of EGFP-H_CN/A with syntaxin. In B EGFP-H_CN stained with rabbit anti-GFP and anti rabbit IgG Alexa Fluor 488. In C syntaxin stained with a monoclonal antibody and anti mouse IgG Alexa Fluor 555. In D the merged images. In A the corresponding bright field.

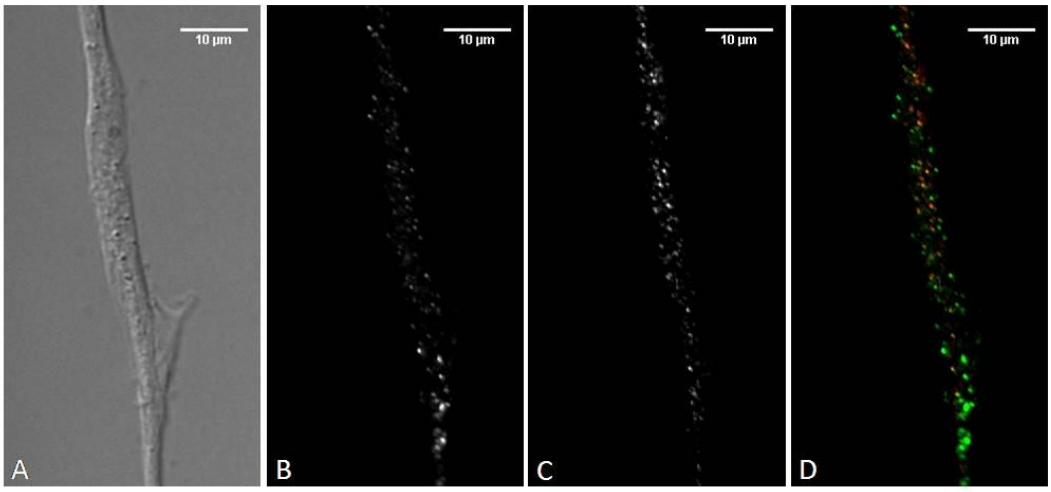

Figure 16 Colocalization of EGFP-H_CN/A with SV2A. In B it is shown EGFP-H_CN/A staining, in C SV2A labelled with a rabbit primary antibody and anti rabbit IgG Alexa Fluor 555 and in D the merged images. In A the corresponding bright field

The rational of these experiments was to investigate whether the H_CN/A subdomain could localize BoNTs on the site of synaptic activity, but it seems

there is no correlation between synaptic activity and EGFP- H_CN/A binding to plasma membrane.

4.4 The N-terminal Half of the Binding Domain of Botulinum Neurotoxin type A Binds to Sphingomyelin-containing Plasma Membrane Microdomains

The plasma membrane of many cells presents microdomains enriched in sphingomyelin, cholesterol and GPI-binding protein, called lipid rafts (Lai, 2003). These particular microdomains have been involved in several cell functions included synaptic vesicle formation (Martin, 2000). It has also been shown that lipid rafts act as specialized domains for tetanus toxin binding and internalization into neurons (Herreros et al., 2001). There are many tools to visualize lipid rafts on plasma membrane. We first of all tried commercial fluorescent B subunit of cholera toxin (Invitrogen) but there was not a high degree of colocalization (not shown). We then used a sphingomyelin binding protein of bacterial origin, Lysenin (Kiyokawa et al., 2005). The first approach was to use commercial active toxin on fixed cells, and to reveal it with rabbit Lysenin anti-serum. Figure 17 shows that the EGFP-H_CN/A and Lysenin staining largely co-localize in HeLa cells, indicating that the microdomains to which the H_CN/A binds are enriched in sphingomyelin.

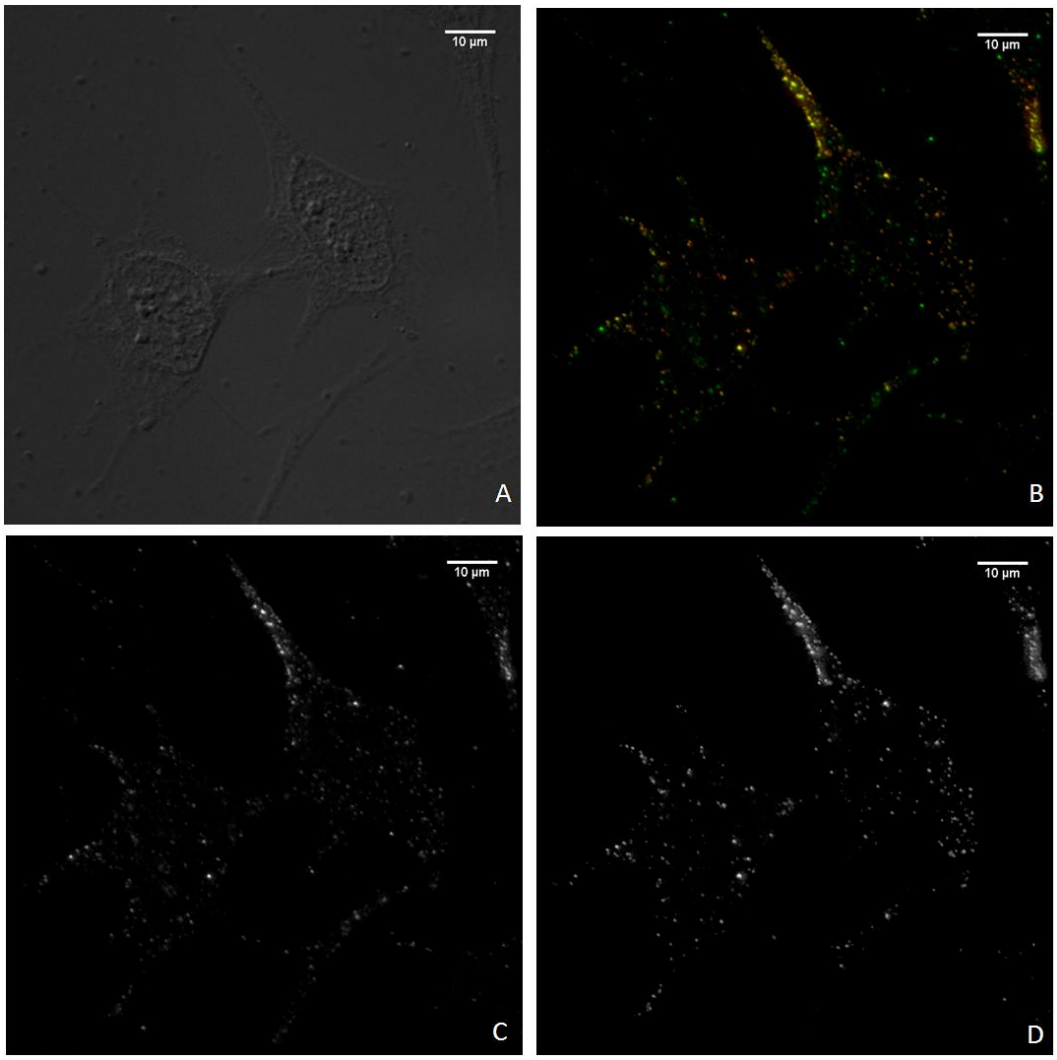

Figure 17. SM enriched domain in HeLa cells stained with commercial Lysenin. HeLa cells were treated with 200 nM of EGFP-H_CN, washed and fixed with cold acetone for 5 minutes. Afterwards cells were incubated for 2h with 1µg/ml of lysenin, a sphingomyelin (SM) specific binding toxin. Lysenin were then stained with lysenin anti-serum and a secondary Alexa555-conjugated antibody. EGFP-H_CN staining is shown in **C**, Lysenin staining in **D**, the merged image in **B** and the corresponding bright field in **A**.

After this initial positive result we decide to improve the experimental condition using only the binding domain of Lysenin fused to Venus fluorescent protein, an improved GFP variant. We made a MTA patent agreement with Prof. T. Kobayashi, who send us the plasmid for the expression of this non toxic sphingomyelin binding protein, named Venus-NT-Lysenin (Ishitsuka et al., 2004). We could then proceed with a co-incubation protocol using mCherry-H_CN/A and

Venus-NT-Lysenin. Figure 18 shows that the mCherry-H_CN/A and Lysenin staining largely co-localize in neuronal and epithelial cells, confirming that the microdomains to which the H_CN/A binds are enriched in sphingomyelin.

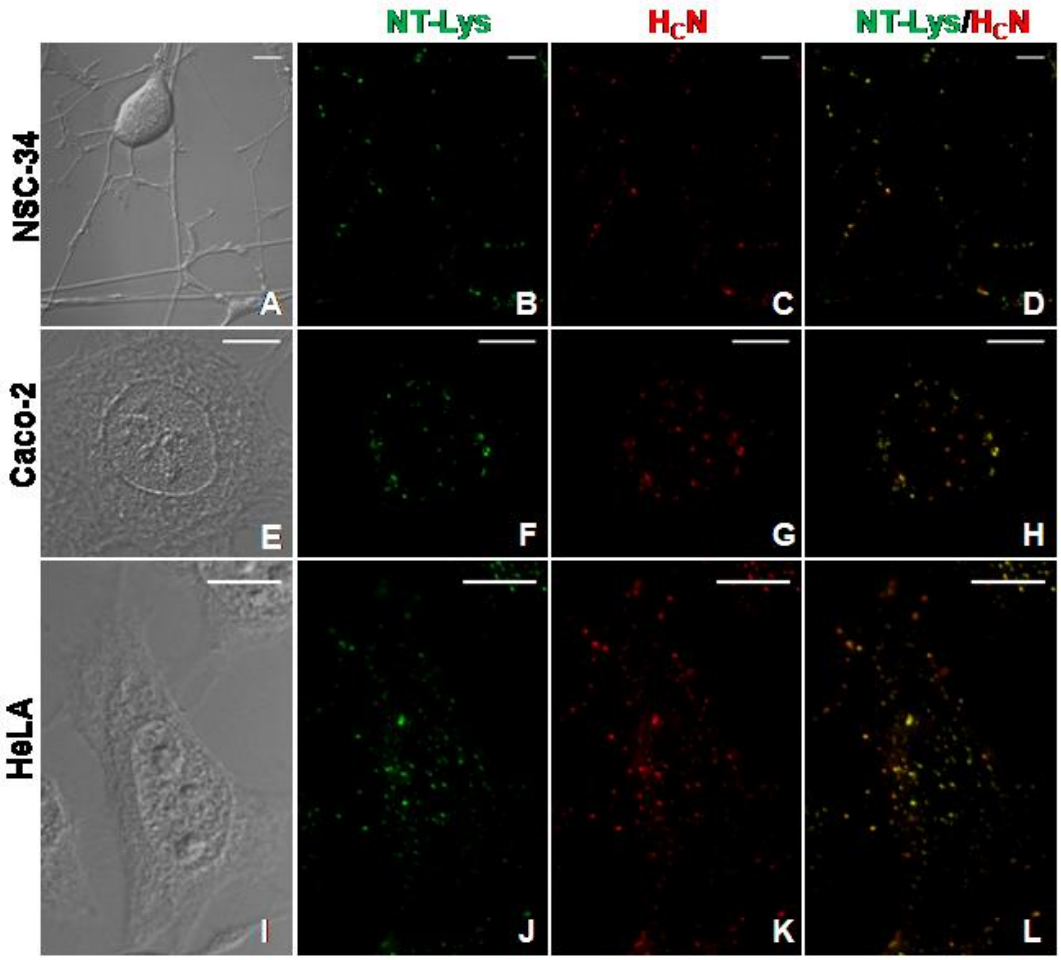

Figure 18 mCherry-H_CN/A colocalizes with sphingomyelin-enriched microdomains of the plasma membrane. Distribution of Venus-NT-Lysenin (B, F, J) which selectively labels sphingomyelin-enriched plasma membrane microdomains and of mCherry-H_CN/A (C, G, K); merged images are shown in D, H, L. This analysis was performed in live, on differentiated NSC-34 (A-D), as well as in fixed Caco-2 (E-H) and HeLa cells (I-L).

The results of these experiments suggest that EGFP-H_CN binds to sphingomyelin-enriched microdomains either on neuronal or epithelial cells. We have performed co-incubation experiments with mCherry-H_CN/A and Venus-NT-Lysenin and they both bind to lipid rafts. We have not performed extensive

studies with different concentrations and protocols to test if there is any competition between these two proteins, but we can say that in the condition we used the binding of Venus-NT-Lysenin does not impede the binding of EGFP-H_CN/A to plasma membrane.

One common critic at immunofluorescence lipid rafts analysis is that fixation step could alter the lipid distribution, but this is not the case because when we performed the experiments on live cells we obtain the same pattern distribution (A-D, figure 18).

4.5 EGFP-H_CN/A Localizes in Detergent-resistant Membrane Microdomains

The first and widely used method to purified lipid rafts is their resistance to detergent, in particular to Triton-X-100 (Hooper, 1999). More recently, it has been shown that different detergents allow to purify different populations of lipids rafts (Pike, 2004), for example inner plasma membrane leaflet components are differentially solubilised by Lubrol WX and Triton X-100 (Delaunay et al., 2008). We decide to try first the classical protocol of lipid rafts purification with a careful solubilisation of the cells with Triton-X-100 and ultracentrifugation purification of the insoluble fractions. We decide to perform the experiments on differentiated NSC-34 cells, because of the difficulty to obtain a sufficient amount of highly pure primary SCMNs cell culture. Figure 19 shows that, indeed, a large part of EGFP-H_CN/A is found in an insoluble fraction together with flotillin, which is a marker of detergent insoluble microdomains. SNAP-25, a palmitoylated plasma

membrane protein, remained concentrated in the bottom fractions of the gradient, which contain the soluble material and the majority of proteins.

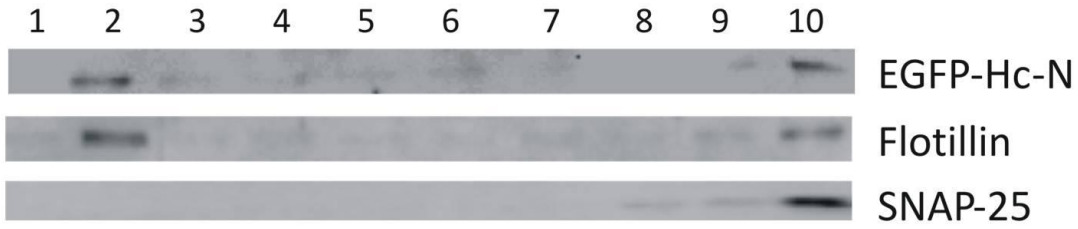

Figure 19 EGFP-H_CN/A localizes in detergent-resistant membrane microdomains. EGFP-H_CN/A is present in the insoluble fraction (lane 2) of the gradient (see MATERIAL AND METHODS), which contains the majority of the microdomain marker flotillin, whilst SNAP-25 is found in soluble fractions (lanes 8-10).

Filatov et. al. have shown that the resistance of cellular membrane antigens to solubilization with Triton X-100 could easily be assessed by flow cytometry analysis (Filatov et al., 2003). This technique has the big advantage to be quantitative, and then we decide to confirm that EGFP-H_CN binds to lipids rafts by FACS analysis. Briefly we adapted the Filatov protocol to ours purpose incubating EGFP-H_CN stained cells with Triton-X-100 at 4°C, in order to solubilize proteins not associated to lipids rafts. We performed several trial experiments with differentiated NSC-34 to set up the experimental conditions; cells were incubated with EGFP-H_CN/A washed, detached, and the fluorescence in the green channel was read. Unfortunately this cellular type, once differentiated, was too sensitive to those treatments and at the end of the experiments most of them were dead. We consequently decide to try HeLa cells to which EGFP-H_CN/A binds as well.

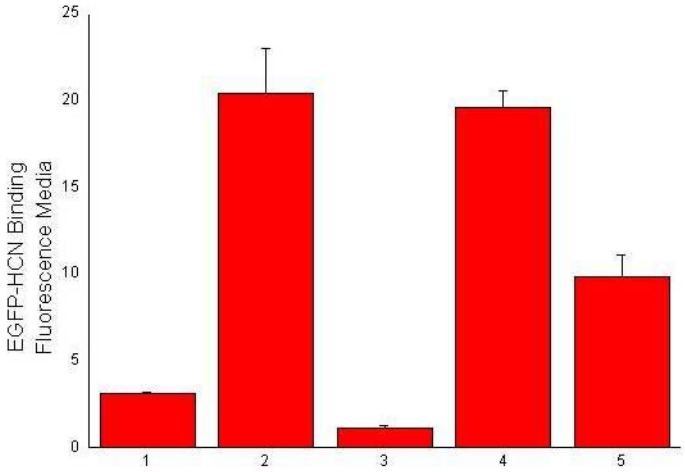

Figure 20 Analysis of the binding of EGFP-H_CN to HeLa by flow cytometry. HeLa cells were incubated with 0.5% BSA in MEM medium (1 and 3) or 250 nM EGFP-H_CN at 37° (2 and 4), or 250 nM EGFP-H_CN at 4°C (5) for 30 minutes. Cells were then washed, detached and samples 3 and 4 were incubated with 1% Triton-X-100 for 30 minutes at 4°C. All the samples were prepared in triplicate and this is one representative experiment. EGFP and EGFP-HC/A did not bind to HeLa cells (not shown).

Figure 20 show that there is no significant fluorescence decrease after the treatment of EGFP-H_CN/A stained cells with Triton-X-100; indeed in samples 2 and 4 the fluorescence media values were comparable, also at the light of the fact that the basal fluorescence of Triton-X-100 treated cells (column 3) is lower than that of control cells. In this experimental set up we investigate also the effect of the temperature on the binding of EGFP-H_CN to cellular plasma membrane. Interesting we found that at 4°C the binding of this protein is lowered by more than 50% (column 5) with respect to 37°C incubation (column 2).

From this group of experiments we can confirm that EGFP-H_CN/A binds to lipids raft and that this interaction is resistant to Triton-X-100 treatment. If we compare the data obtained for NSC-34 lipid rafts purification and for HeLa cells FACS analysis we notice that in the first case the major part of EGFP-H_CN/A is

retained in lipid raft but that a portion of the protein is solubilised, whereas in the second case there is almost no fluorescence decrease after Triton-X-100 treatment (Triton-X-100 concentrations and incubation time were the same). This could be due to the overall different experimental procedures or to a differential resistance at solubilisation of HeLa or NSC-34 lipid rafts.

We have shown that the EGFP-H_CN/A binding to plasma membrane is inhibited at 4°C. A possible explanation is that a lipid structure reorganization is necessary for the binding and that such process is slow down by the reduced lipids mobility at 4°C. It is also possible that an active endocytic-exocytic pathway is needed for EGFP-H_CN/A binding to occur, maybe for the exposure of a possible receptor.

4.6 Effect of Lipid Raft Perturbing Agents on EGFP-H_CN/A Binding to HeLa Cells

There are many tools to perturb the plasma membrane rafts organization; the major group acts on plasma membrane cholesterol: methyl-β-cyclodextrin is a cyclic oligosaccharides consisting of 7 glucopyranose units and has the propriety to extract cholesterol from membranes. Cholesterol oxidase modify a hydroxyl group essential for sphingomyelin interaction changing lipid rafts proprieties; etc... While some compounds act on other lipids, for example SMase hydrolyses sphingomyelin in ceramide and phosphocholine. It has been shown that different lipid rafts populations have different susceptibility to these agents, using several of them it is thus possible to characterize the rafts population that are involved in EGP-H_CN/A binding. The first approach was with fluorescent microscopy, but it

became soon evident the difficulty in evaluating and comparing the effect of the different treatments. We decide then to continue this investigation on HeLa cells by flow cytometry: this method gives quantitative results, allows the evaluation of cell death and the elimination of their contribute to overall fluorescence measure. In figure 21 it is shown an exemplificative panel with control cells (A-C); EGFP-H_CN stained cells (D-F); SMase treated and EGFP-H_CN stained cells (G-I). Comparing panel I with panel F is evident that the number of cells (events) with a high fluorescence ($>10^2$) is decreased by SMase treatment; whereas comparing panel H with panel B there is no evident changing in PI fluorescence, in particular the R3 (death cells) populations are similar.

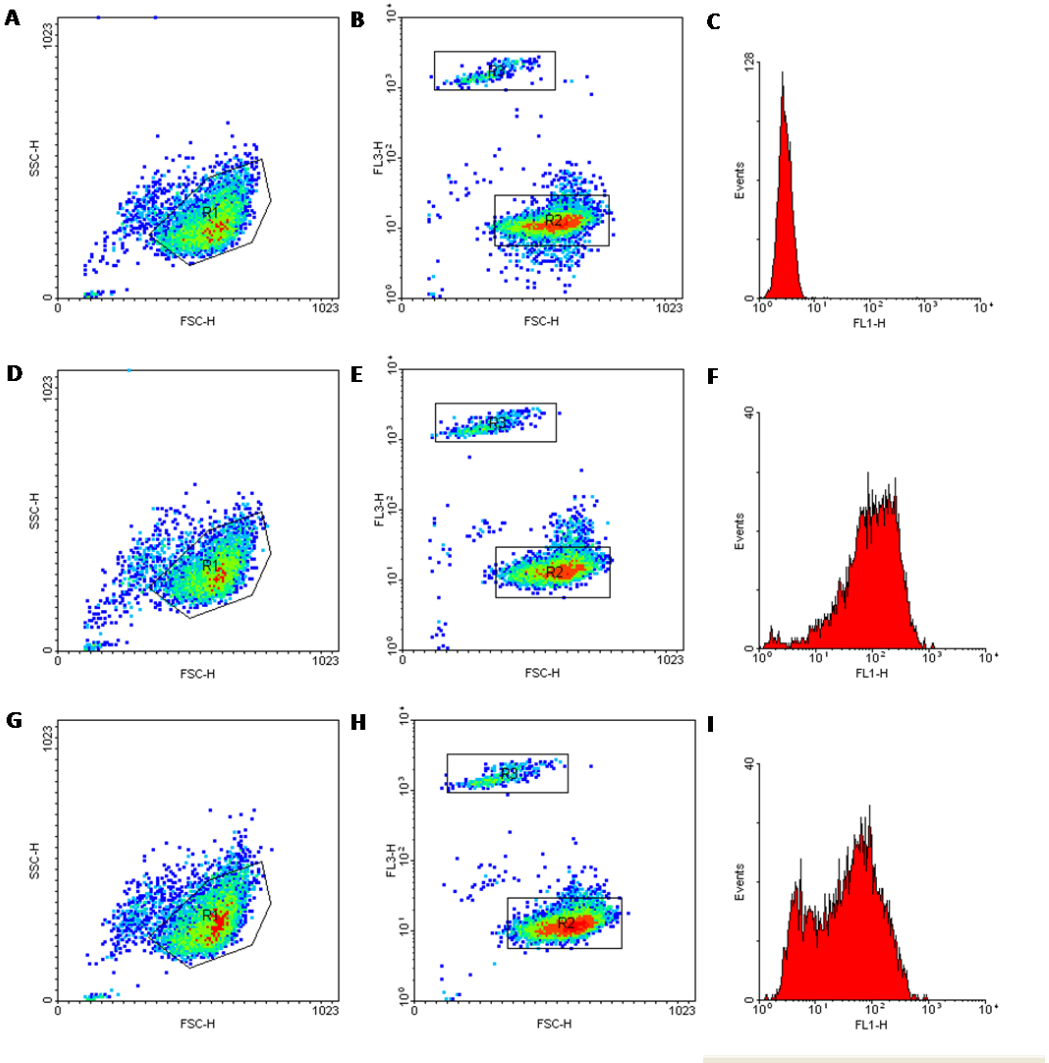

Figure 21 Density and histogram plots of HeLa cells treated with SMase and incubated with EGFP-H_CN/A. Cells were analyzed for size (forward scatter-height, FSC-H) and complexity (side (90°) scatter-height, (SSC-H) panel A,D,G and R1 is the selected population; the vitality was evaluated with propidium iodine fluoresce (FL3-H panel B, E, H, R3 correspond to dead cells and R2 is the selected population); only the contribution of gated cells (belonging to both R1 and R2) was counted for the fluorescence in the green channel (FL1-H, panel C, F, I). In the upper three panels there are shown data relative to control cells, in the middle, data relative to 1 μM EGFP-H_CN/A incubation and in the bottom tree panels, data relative to cells pre-incubated with SMase and then with 1 μM EGFP-H_CN/A. SMase treatment did not alter basal cell fluorescence (not shown).

In figure 22 are summarized the effects of all the treatments on EGFP-H_CN/A (panel A) and Venus-NT-Lysenin (panel B).

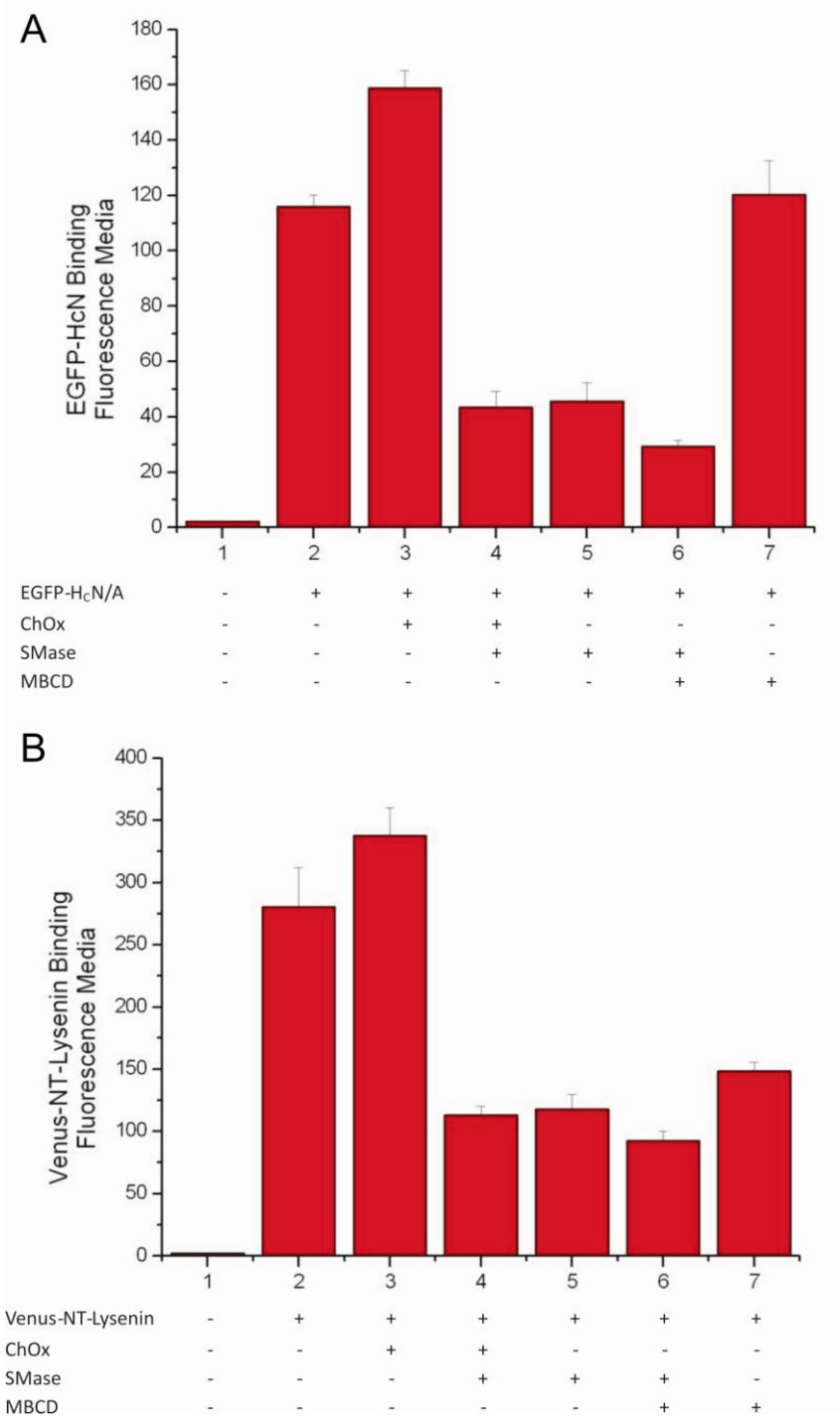

Figure 22. Effect of lipid rafts perturbation in HeLa cells. HeLa cells were incubated with 0.5%BSA in MEM medium (1a e 1b) or 1 μM EGFP-H_CN (2-7 panel a), or 1 μM Venus-NT-lysenin (2-7 panel b) in the same media. Cells were pre-incubate with: ChOx (Cholesterol Oxidise) 1u/ml 2h a 37°C (3); ChOx 1u/ml 2h a 37°C and SMase (sphingomyelinase) 0,5 u/ml 1h a 37°C (4); SMase 0,5 u/ml 1h a 37°C (5); 2.5 mM MBCD 1h a 37°C and SMase 0,5 u/ml 1h a 37°C (6); 2.5 mM MBCD 1h a 37°C (7). This representative experiment shows that SMase lower the EGFP-H_CN/A chimera binding to the cell membrane. The experiments were perform in parallel with Venus-NT-lysenin, as a control, and gave the expected results.

It has already been published that the binding of Venus-NT-Lysenin is affected by pre-treatment with SMase and MBCD (Kiyokawa et al., 2005), thus we used the decrease of Venus-NT-Lysenin binding to the cells as a control of the efficacy of lipid rafts modification. We obtained the expected results for SMase and MBCD, the unexpected results was an increase of the binding consequent to ChOx pre-incubation (Panel B of figure 22). When multiple treatments were combined there is no evidence of synergistic effects. In panel A the results on EGFP-H_CN/A binding are shown: SMase pre-incubation shows almost the same effect on EGFP-H_CN/A that for Venus-NT-Lysenin; interestingly the binding of H_CN seems to be less affected of thus of Lysenin by MBCD treatment; ChOx pre-incubation gives the same unexpected increase for EGFP-H_CN/A, and there is not a synergistic effects of the treatments.

From this group of evidences we can concluded that the EGFP-H_CN/A binding is affected by SMase treatment as the sphingomyelin binding toxin Lysenin, but is less affected than Lysenin by plasma membrane cholesterol extraction. The data relative to ChOx could be interpreted as a lipid rafts structure reorganization that finally favours the binding of EGFP-H_CN/A and, in a less significative way, that of Venus-NT-Lysenin.

4.7 H_CN/A Interacts with Phospholipid Monolayers

The previous experiments have clearly shown that lipids rafts are involved in the binding of EGFP-H_CN/A to the plasma membrane. We decide to investigate if this BoNT/A subdomain was able to directly bind to one of the lipid component of lipid rafts. We have shown that EGFP-H_CN/A colocalizes with a the

sphingomyelin binding toxin Lysenin and that treatment with a SMase lower the binding of EGFP-H_CN/A to the plasma membrane, thus sphingomyelin seems to be the more attractive lipid receptor. We decided to use the system of lipid planar monolayer that have been used with success to show that TeNT interact with lipid monolayer of different compositions (Schiavo et al., 1991). In particular TeNT binds to DOPC monolayers and inserts into the phospholipid layer at neutral pH. This effect is potentiated by acidic phospholipids without an apparent preference for a single a class of phospholipids. Polysialoglycosphingolipids further increase the fixation and penetration of tetanus toxin in lipid monolayers, but no specific requirement for a particular ganglioside was identified. The penetration of tetanus toxin in the lipid monolayer is pH dependent, it increases with lowering pH. We decide to look at the interaction of the whole BoNT/A with lipid monolayers, and we chose a lipid composition that mimic that of lipid rafts (DOPC:SM:Ch, 50:30:20) enriched in a ganglioside mixture (DOPC:SM:Ch:G, 45:30:20:5). Consistent with what has been shown for TeNT there is an interaction at neutral pH that is significantly increased by acidification (Figure 23).

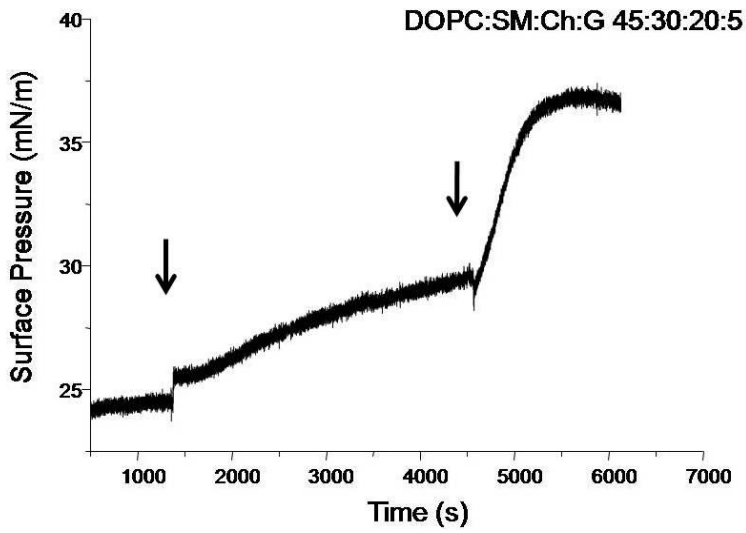

Figure 23. BoNT/A interaction with lipid monolayer with lipid raft like composition supplement with a mixture of ganglioside. The first arrow correspond to the injection of BoNT/A to a final concentration of 34 nM, the second arrow correspond to injection of phosphoric acid to lower the pH for 7.4 to 5. The pressure increment means that the protein interacts with the lipid monolayer.

Then we decided to investigate the interaction of recombinant H_CN with lipid monolayer of an increasing complexity, from mono-component DOPC monolayer to a lipid raft tri-component monolayer. We did not add gangliosides because this binding site is on the H_CC portion.

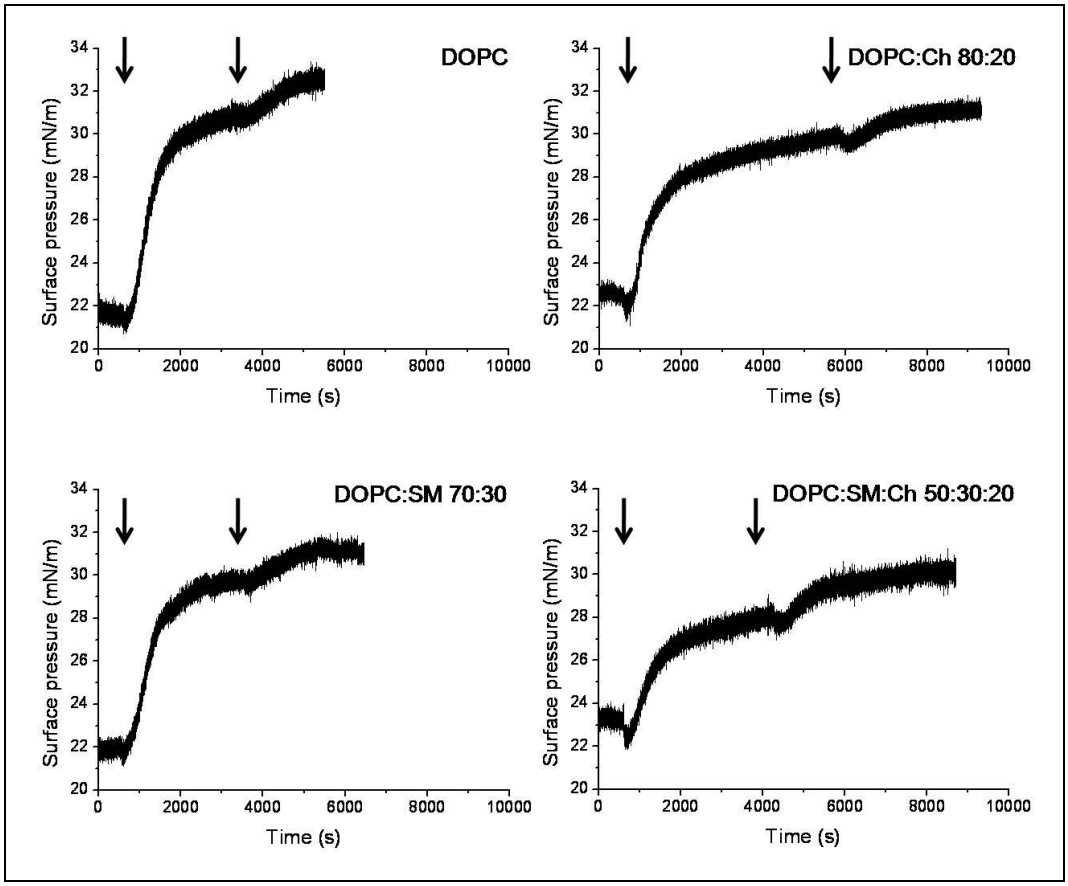

Figure 24 Binding of recombinant H_CN to lipid monolayers of growing complexity.

The protein has been injected in a 600 µl chamber overlaid by lipid monolayer to the final concentration of 34 nM. Different lipid compositions have been tested and are indicated in the figure. The first arrow of each panel indicates H_CN addition the second arrow the acidification to pH 5 with phosphoric acid.

Figure 24 shows that the H_CN itself is able to interact with lipid monolayers: as for TeNT and BoNT/A there is an interaction at neutral pH, and a further interaction due to acidification. If we confront the entity of this two increments, it seems that for H_CN/A the majority of the binding is achieved already at neutral pH, whereas for BoNT/A the acid pH is fundamental for the interaction. We can speculate that H_CN/A contain a lipid interaction site, hide in the neutral BoNT/A conformation, that needs acidification to be exposed; on the contrary in the H_CN/A recombinant protein this site is always exposed. If we consider the effect

of the increasing lipid complexity of the monolayer, H_CN/A bind to DOPC as well to more complex monolayer. In particular the addiction of SM, either in presence or absence of Ch, does not increase the binding of H_CN/A.

4.8 The N-terminal Half of the Binding Domain of Botulinum Neurotoxin Type A Binds to Phosphatidylinositol Phosphate on Lipid Dot Blot

We decided to try to identify possible specific interactions of H_CN/A with defined lipids by using, the well established dot-blot binding assay. In this assay various lipids are dotted on nitrocellulose paper stripes. We to used the EGFP-H_CN/A chimera for the possibility of detect and amplified the signal of bound protein with a polyclonal anti-GFP antibody. Control experiment performed with EGFP showed no binding, thus we can ascribe the binding of EGFP-H_CN/A to the H_CN/A subdomain. As shown in figure 25A, there is a defined interaction with negatively charged phospholipids PA and PS; however, H_CN/A display a much stronger interaction with PI(4)P. The lack of interaction with SM is only apparently in contradiction with the findings of paragraphs 4.4 and 4.6 because those assays only showed the involvement of SM enriched lipids rafts in the EGFP-H_CN/A binding to plasma membrane, not a direct interaction with SM. To scrutinize the interaction within the PIPs family, a specific assay was carried out (Figure 25B).

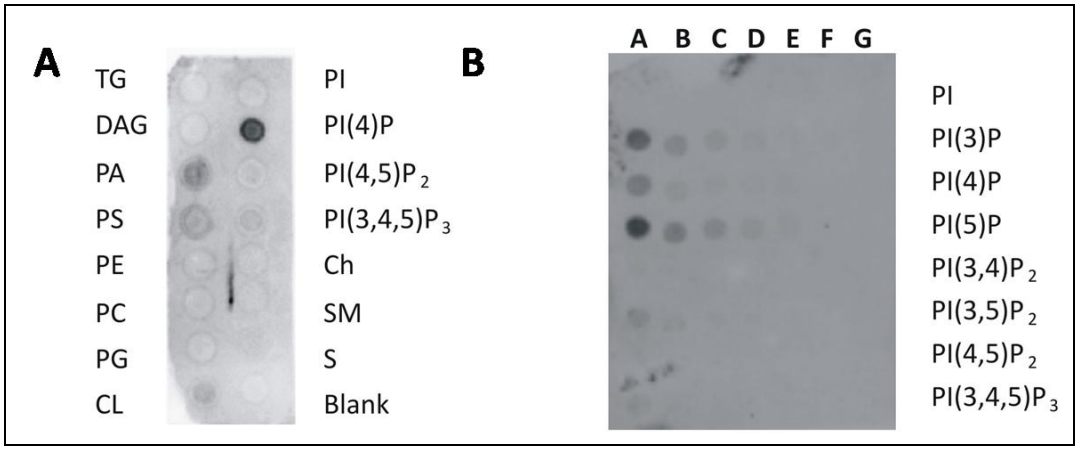

Figure 25 EGFP-H_CN/A binding to membrane lipids dot blot. EGFP-H_CN/A binds preferentially to PI(5)P with small or no affinity to PI, PIP2 and PIP3; different amounts of lipids are spotted in different columns: A, 100 nmol/spot; B, 50 nmol/spot; C, 25 nmol/spot; D, 12.5 nmol/spot; E, 6.25 nmol/spot; F, 3.13 nmol/spot; G, 1.56 nmol/spot.

The result indicates that H_CN/A is capable of interacting with all PI monophosphate, particularly with the 5 isomer. The 3 and 4 isomers are recognized as well but less strongly. In agreement with these data, EGFP-H_CN/A also binds to PI(3,5)P_2, but with a weak affinity. It is noteworthy that, using the same approach, it was recently reported that BoNT/D and Hc/D bind to PE (Tsukamoto et al., 2008).

4.9 Bioinformatical Considerations

Lipid-binding proteins are diverse in sequence, structure, and function, non-the-less, lipid recognition by proteins is primarily mediated by some combination of a number of structural and physicochemical features including conserved fold elements, specific lipid-binding site architectures and recognition motif, ordered hydrophobic and polar contacts between lipids and proteins, and multiple noncovalent interactions from proteins residues to lipid head groups and hydrophobic tails. Many efforts have been done to develop software able to

predict new lipid interaction site and novel lipid binding proteins (Lin et al., 2006), but until now we still need a visual inspection of available crystallographic data to find out a possible similarity. Many PIPs binding proteins are known (Balla, 2005), and at this point we started to compare their sequences and crystallographic structures with those of the BoNTs. Indeed, we found a 27.5% sequence identity among the H_CN of BoNT/A and a PI(5)P binding protein, termed the inhibitor of growth family member 2 (ING2). Furthermore this protein gives almost the same results of EGFP-H_CN/A in a similar dot blot assay (Gozani et al., 2003). Figure 26 shows that there is also a structural similarity between ING2 (Kutateladze and Overduin, 2001) and BoNT/A (figure 26). On this basis, we identify a putative inositol phosphate binding site in the BoNT/A region comprised between amino acid Ser-876 and Lys-929 which correspond to a β-prism. It is also possible that the four positively charged residues of BoNT/A, Arg-892, Lys-896, Lys-902, Lys-910, are involved in PIP binding. Consistent with this putative site of the PIP interaction, a peptide that inhibits the binding of BoNT/A to synaptosome and a toxin neutralizing antibody (Levy et al., 2007; Maruta et al., 2004) map in this portion of BoNT/A (figure 26). Furthermore, the side chains of several tryptophans (945, 1013, 1067, 1100, 1290) face toward this site and tryptophans are known to play frequently important roles in membrane interaction (Jin et al., 2003; Kwiatkowska et al., 2007).

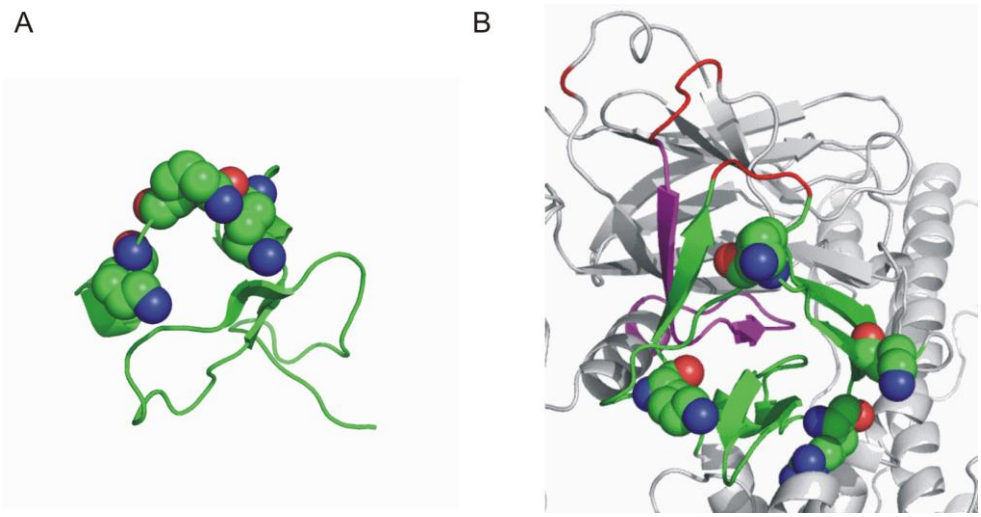

Figure 26 A. H_CN/A similarity with PIP binding protein. The structure of ING2 (modelled on ING1 structure PBD 2QIC, sequence identity 88%) and **B.** putative BoNT/A. lipid binding sites are shown as cartoons in green. The positively charged residues of ING2 (Lys-49, Lys-51, Lys-53), known to interact with the phosphorus groups (Gozani et al., 2003), and the positively charged residues (Arg-892, Lys-896, Lys-902, Lys-910) of BoNT/A, possibly involved in the binding are shown as spheres. For BoNT/A (b) the remaining structures is shown in grey with in magenta a peptide (residues 1065-1083) that block the binding of BoNT/A to synaptosome (Maruta et al., 2004) whilst in red is the site of interaction of another neutralizing antibody (Levy et al., 2007).

The 876-929 segment of BoNT/A is not highly conserved among serotypes, but it is possible that different lipids may be involved in the promotion of the membrane interaction of different neurotoxins, as indicated by the BoNT/D binding to PE (Tsukamoto et al., 2005). We suggest that these additional interactions with the membrane surface may play the role of positioning the toxin on the membrane surface ready for membrane insertion, as it is illustrated in figure 27. The model suggests that the H_CN sub-domain has the role of bringing the membrane translocating domain HN close to the membrane surface, possibly close to areas of lipid mismatching (as those present at the boundaries of membrane microdomains) to facilitate its membrane penetration. The double, ganglioside and PIP, lipid binding places the HN segment 620-680 close to the membrane surface, ready for insertion into the lipid bilayer. Further studies are

clearly required to demonstrate that this is indeed the first part of the toxin which inserts into the membrane, but it is noteworthy that this segment is highly conserved. This suggestion can be tested using the available highly sensitive membrane translocation assay of BoNT (Fischer and Montal, 2007) and other biophysical methods.

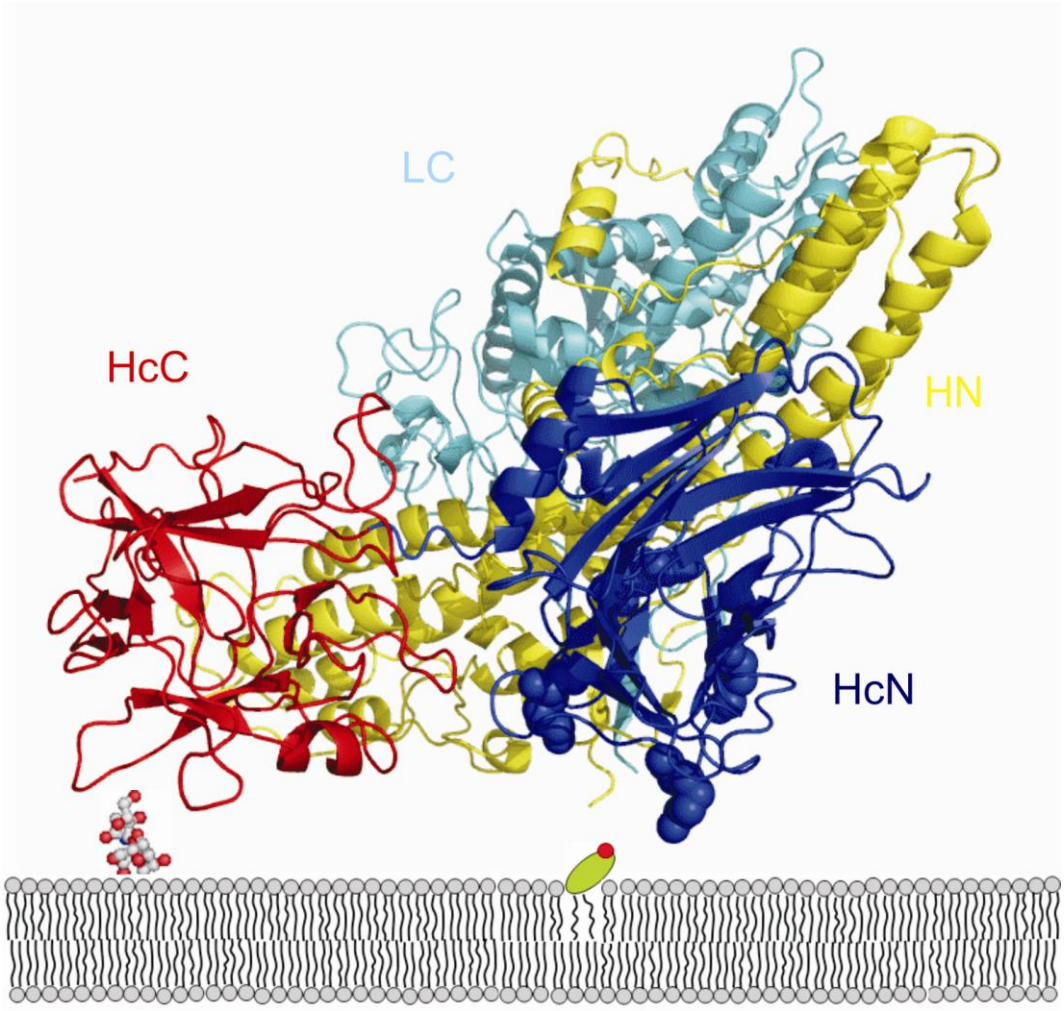

Figure 27 A model of BoNT/A bound to plasma membrane based on the interaction of the binding domain with a polysialoganglioside and a PIP molecule. BoNT/A ribbon diagram with subdomains labeled with H_CC (red), H_CN (blue), HN (yellow) and LC (light blue). Simultaneous binding of BoNT/A to the oligosaccharide moiety of a polysialoganglioside (left hand side, in grey and red) and PIP (right hand side, with inositol in green and phosphate in red) imposes a rotation of the HN and LC domains that position the HN segment 620-680 close to the membrane surface. The HCN positive charged residues Arg-892, Lys-896, Lys-902, Lys-910, which are suggested to play a major role in the interaction with PIP, are shown as spheres.

5 CONCLUSIONS

The aim of the thesis was to investigate the H_CN subdomain contribution to the extraordinary potency of the CNT toxin family. First of all we were able to observe the binding of H_CN/A to plasma membrane with fluorescent microscopy, on fixed and on live cells, using EGFP as well mCherry H_CN/A chimera. Those chimeras bind to the plasma membrane of the neuronally differentiated NSC-34 cells and to spinal cord motoneurons (figure 10); in both cases, the binding is distributed all along the cell surface in discrete spots. Surprisingly, fluorescent H_CN/A not only binds to neurons, but also to the plasma membrane of epithelial cells with the same discrete and spotty binding (figure 13). Its cell surface distribution was never followed by internalization, as indicated by: a) its morphological distribution (figure 12), b) no fluorescence quenching due to exposure of the EGFP moiety to acid endosomal lumen (not shown), and c) coincidence of the EGFP-H_CN/A stainings obtained with an anti-GFP antibody with or without membrane permeabilization (figure 11). These data suggest that H_CN/A binds to cells with no internalization. With respect to the ability of this toxin subdomain to bind epithelial cells we investigate if H_CN was sufficient to mediate the transcytosis through intestine derived cell line monolayers. We were able to repeat transcytosis experiments of the whole binding HC of BoNT/A fused to EGFP, but in the same conditions we have not observed transcytosis of EGFP-H_CN/A (figure 14). Thus the first conclusion is that H_CN/A has a general cell binding activity common to neuronal and non neuronal cells, but that this binding is not followed by internalization or transcytosis.

The characteristic spotty binding of EGFP-H_CN/A suggested that the process may be mediated by discrete plasma membrane microdomains. In agreement with this hypothesis we found: a high level of colocalization with the sphingomyelin-enriched lipid raft marker, lysenin (figure 17,18); that EGFP-H_CN/A localizes in insoluble fraction after Triton-X-100 treatment and ultracentrifugation of NSC-34 cells (figure 19); and that Triton-X-100 does not decreases the bound EGFP-H_CN/A to HeLa cells measured by flow cytometry (figure 20). The second conclusion is the involvement of lipid raft in the binding, in particular a subpopulation enriched in sphingomyelin. These lipid rafts are highly sensitive to SMase treatment, as it shown with flow cytometry measurement of EGFP-H_CN/A binding on HeLa cells (figure 21, 22).

We have then start to investigate the possibility of a direct binding of H_CN/A subdomain to lipids. With lipid monolayer system we have shown that H_CN/A is able to bind to DOPC monolayer, the binding occurs at neutral pH and it is further incremented by acidification. When the complexity of the lipid mixture was increased to resemble that of lipid raft (DOPC-SM-Ch) H_CN/A did not show a preferential binding (figure 24). This was the first clue that even if SM-enriched lipid rafts are involved, there are not direct binding of EGFP-H_CN/A to SM. We further investigate the possibility of a binding to a specific lipid with dot-blot assay. We found a define interaction of EGFP-H_CN/A with negative lipid as phosphatidic acid and phosphatidylserine, but much more stronger with phosphatidylinositol phosphate, in particular with the 5 isomer (PI(5)P) (figure 25). Bioinformatical analysis allow to identify BoNT/A region comprised between amino acid Ser-876 and Lys-929 as a putative binding site to phosphatidylinositol

monophosphates (PIPs) (figure 26). The family of phosphoinositides are important mediators of cellular response to growth factors and in vesicular trafficking (Vicinanza et al., 2008), also at synapse (Cremona and De Camilli, 2001). They are enriched in the cytosolic leaflet of the plasma membrane, but it is possible that they are present on the cell surface in association with SM-containing microdomains. In fact, PIPs were found to localize in SM-enriched domain in the presence of cholesterol (Kinoshita, 2008). Thus the third conclusion is that H_CN/A interact with PIPs, and that this interaction together with that of ganglioside could contribute to place the HN segment in an insertion competent orientation (figure 27).

In order to characterize BoNT/A binding site to PIPs a mutagenesis analysis of the suggested involved positively charged residues is necessary. Furthermore a comparison with the H_CN domain of other BoNTs will greatly contribute to the knowledge of this toxin family.

REFERENCES

Agarwal, R., Binz, T., and Swaminathan, S. (2005). Structural analysis of botulinum neurotoxin serotype F light chain: implications on substrate binding and inhibitor design. Biochemistry *44*, 11758-11765.

Agarwal, R., Eswaramoorthy, S., Kumaran, D., Binz, T., and Swaminathan, S. (2004). Structural analysis of botulinum neurotoxin type E catalytic domain and its mutant Glu212-->Gln reveals the pivotal role of the Glu212 carboxylate in the catalytic pathway. Biochemistry *43*, 6637-6644.

Aoki, K. R. (2001). A comparison of the safety margins of botulinum neurotoxin serotypes A, B, and F in mice. Toxicon *39*, 1815-1820.

Arndt, J. W., Chai, Q., Christian, T., and Stevens, R. C. (2006). Structure of botulinum neurotoxin type D light chain at 1.65 A resolution: repercussions for VAMP-2 substrate specificity. Biochemistry *45*, 3255-3262.

Arndt, J. W., Yu, W., Bi, F., and Stevens, R. C. (2005). Crystal structure of botulinum neurotoxin type G light chain: serotype divergence in substrate recognition. Biochemistry *44*, 9574-9580.

Bade, S., Rummel, A., Reisinger, C., Karnath, T., Ahnert-Hilger, G., Bigalke, H., and Binz, T. (2004). Botulinum neurotoxin type D enables cytosolic delivery of enzymatically active cargo proteins to neurones via unfolded translocation intermediates. J Neurochem *91*, 1461-1472.

Bajjalieh, S. M., Peterson, K., Shinghal, R., and Scheller, R. H. (1992). SV2, a brain synaptic vesicle protein homologous to bacterial transporters. Science *257*, 1271-1273.

Baldwin, M. R., and Barbieri, J. T. (2007). Association of botulinum neurotoxin serotypes a and B with synaptic vesicle protein complexes. Biochemistry *46*, 3200-3210.

Balla, T. (2005). Inositol-lipid binding motifs: signal integrators through protein-lipid and protein-protein interactions. J Cell Sci *118*, 2093-2104.

Billante, C. R., Zealear, D. L., Billante, M., Reyes, J. H., Sant'Anna, G., Rodriguez, R., and Stone, R. E., Jr. (2002). Comparison of neuromuscular blockade and recovery with botulinum toxins A and F. Muscle Nerve *26*, 395-403.

Binz, T., Bade, S., Rummel, A., Kollewe, A., and Alves, J. (2002). Arg(362) and Tyr(365) of the botulinum neurotoxin type a light chain are involved in transition state stabilization. Biochemistry *41*, 1717-1723.

Black, J. D., and Dolly, J. O. (1986). Interaction of 125I-labeled botulinum neurotoxins with nerve terminals. II. Autoradiographic evidence for its uptake into motor nerves by acceptor-mediated endocytosis. J Cell Biol *103*, 535-544.

Bleck, E. (1989). Clinical aspects of tetanus. In: Simpson LL (ed) Botulinum neurotoxin and tetanus toxin. . Academic Press, San Diego, CA,, pp 379–398.

Bohnert, S., and Schiavo, G. (2005). Tetanus Toxin Is Transported in a Novel Neuronal Compartment Characterized by a Specialized pH Regulation. J Biol Chem *280*, 42336-42344.

Breidenbach, M. A., and Brunger, A. T. (2004). Substrate recognition strategy for botulinum neurotoxin serotype A. Nature *432*, 925-929.

Breidenbach, M. A., and Brunger, A. T. (2005). 2.3 A crystal structure of tetanus neurotoxin light chain. Biochemistry *44*, 7450-7457.

Brin, M. F. (1997). Botulinum toxin: chemistry, pharmacology, toxicity, and immunology. Muscle Nerve Suppl *6*, S146-168.

Brin, M. F., Lew, M. F., Adler, C. H., Comella, C. L., Factor, S. A., Jankovic, J., O'Brien, C., Murray, J. J., Wallace, J. D., Willmer-Hulme, A., and Koller, M. (1999). Safety and efficacy of NeuroBloc (botulinum toxin type B) in type A-resistant cervical dystonia. Neurology *53*, 1431-1438.

Bruns, D., Engers, S., Yang, C., Ossig, R., Jeromin, A., and Jahn, R. (1997). Inhibition of transmitter release correlates with the proteolytic activity of tetanus toxin and botulinus toxin A in individual cultured synapses of Hirudo medicinalis. J Neurosci *17*, 1898-1910.

Bullens, R. W., O'Hanlon, G. M., Wagner, E., Molenaar, P. C., Furukawa, K., Furukawa, K., Plomp, J. J., and Willison, H. J. (2002). Complex gangliosides at the neuromuscular junction are membrane receptors for autoantibodies and botulinum neurotoxin but redundant for normal synaptic function. J Neurosci *22*, 6876-6884.

Bullough, P. A., Hughson, F. M., Treharne, A. C., Ruigrok, R. W., Skehel, J. J., and Wiley, D. C. (1994). Crystals of a fragment of influenza haemagglutinin in the low pH induced conformation. J Mol Biol *236*, 1262-1265.

Chaddock, J. A., Purkiss, J. R., Duggan, M. J., Quinn, C. P., Shone, C. C., and Foster, K. A. (2000). A conjugate composed of nerve growth factor coupled to a non-toxic derivative of Clostridium botulinum neurotoxin type A can inhibit neurotransmitter release in vitro. Growth Factors *18*, 147-155.

Chai, Q., Arndt, J. W., Dong, M., Tepp, W. H., Johnson, E. A., Chapman, E. R., and Stevens, R. C. (2006). Structural basis of cell surface receptor recognition by botulinum neurotoxin B. Nature *444*, 1096-1100.

Chen, R., Karp, B. I., and Hallett, M. (1998). Botulinum toxin type F for treatment of dystonia: long-term experience. Neurology *51*, 1494-1496.

Chen, S., and Barbieri, J. T. (2006). Unique substrate recognition by botulinum neurotoxins serotypes A and E. J Biol Chem *281*, 10906-10911.

Chen, S., Kim, J. J., and Barbieri, J. T. (2007). Mechanism of substrate recognition by botulinum neurotoxin serotype A. J Biol Chem *282*, 9621-9627.

Couesnon, A., Pereira, Y., and Popoff, M. R. (2008). Receptor-mediated transcytosis of botulinum neurotoxin A through intestinal cell monolayers. Cell Microbiol *10*, 375-387.

Cremona, O., and De Camilli, P. (2001). Phosphoinositides in membrane traffic at the synapse. J Cell Sci *114*, 1041-1052.

Critchley, D. R., Nelson, P. G., Habig, W. H., and Fishman, P. H. (1985). Fate of tetanus toxin bound to the surface of primary neurons in culture: evidence for rapid internalization. J Cell Biol *100*, 1499-1507.

Deinhardt, K., Berninghausen, O., Willison, H. J., Hopkins, C. R., and Schiavo, G. (2006). Tetanus toxin is internalized by a sequential clathrin-dependent mechanism initiated within lipid microdomains and independent of epsin1. J Cell Biol *174*, 459-471.

Delaunay, J. L., Breton, M., Trugnan, G., and Maurice, M. (2008). Differential solubilization of inner plasma membrane leaflet components by Lubrol WX and Triton X-100. Biochim Biophys Acta *1778*, 105-112.

Dolly, J. O., Black, J., Williams, R. S., and Melling, J. (1984). Acceptors for botulinum neurotoxin reside on motor nerve terminals and mediate its internalization. Nature *307*, 457-460.

Dong, M., Richards, D. A., Goodnough, M. C., Tepp, W. H., Johnson, E. A., and Chapman, E. R. (2003). Synaptotagmins I and II mediate entry of botulinum neurotoxin B into cells. J Cell Biol *162*, 1293-1303.

Dong, M., Yeh, F., Tepp, W. H., Dean, C., Johnson, E. A., Janz, R., and Chapman, E. R. (2006). SV2 is the protein receptor for botulinum neurotoxin A. Science *312*, 592-596.

Dressler, D., and Bigalke, H. (2005). Botulinum toxin type B de novo therapy of cervical dystonia: frequency of antibody induced therapy failure. J Neurol *252*, 904-907.

Dressler, D., and Eleopra, R. (2006). Clinical use of non-A botulinum toxins: botulinum toxin type B. Neurotox Res *9*, 121-125.

Duchen, L. W. (1971). An electron microscopic study of the changes induced by botulinum toxin in the motor end-plates of slow and fast skeletal muscle fibres of the mouse. J Neurol Sci *14*, 47-60.

Eleopra, R., Tugnoli, V., Rossetto, O., De Grandis, D., and Montecucco, C. (1998). Different time courses of recovery after poisoning with botulinum neurotoxin serotypes A and E in humans. Neurosci Lett *256*, 135-138.

Evans, E. R., Sutton, J. M., Gravett, A., and Shone, C. C. (2005). Analysis of the substrate recognition domain determinants of botulinum type B toxin using phage display. Toxicon *46*, 446-453.

Fang, H., Luo, W., Henkel, J., Barbieri, J., and Green, N. (2006). A yeast assay probes the interaction between botulinum neurotoxin serotype B and its SNARE substrate. Proc Natl Acad Sci U S A *103*, 6958-6963.

Fernandez-Salas, E., Steward, L. E., Ho, H., Garay, P. E., Sun, S. W., Gilmore, M. A., Ordas, J. V., Wang, J., Francis, J., and Aoki, K. R. (2004). Plasma membrane localization signals in the light chain of botulinum neurotoxin. Proc Natl Acad Sci U S A *101*, 3208-3213.

Filatov, A. V., Shmigol, I. B., Kuzin, II, Sharonov, G. V., and Feofanov, A. V. (2003). Resistance of cellular membrane antigens to solubilization with Triton X-100 as a marker of their association with lipid rafts--analysis by flow cytometry. J Immunol Methods *278*, 211-219.

Fischer, A., and Montal, M. (2007). Single molecule detection of intermediates during botulinum neurotoxin translocation across membranes. PNAS *104*, 10447-10452.

Foran, P., Lawrence, G. W., Shone, C. C., Foster, K. A., and Dolly, J. O. (1996). Botulinum neurotoxin C1 cleaves both syntaxin and SNAP-25 in intact and permeabilized chromaffin cells: correlation with its blockade of catecholamine release. Biochemistry *35*, 2630-2636.

Galazka, A., and Gasse, F. (1995). The present status of tetanus and tetanus vaccination. Curr Top Microbiol Immunol *195*, 31-53.

Gozani, O., Karuman, P., Jones, D. R., Ivanov, D., Cha, J., Lugovskoy, A. A., Baird, C. L., Zhu, H., Field, S. J., Lessnick, S. L., *et al.* (2003). The PHD finger of the chromatin-associated protein ING2 functions as a nuclear phosphoinositide receptor. Cell *114*, 99-111.

Hanna, P. A., Jankovic, J., and Vincent, A. (1999). Comparison of mouse bioassay and immunoprecipitation assay for botulinum toxin antibodies. J Neurol Neurosurg Psychiatry *66*, 612-616.

Hanson, M. A., and Stevens, R. C. (2000). Cocrystal structure of synaptobrevin-II bound to botulinum neurotoxin type B at 2.0 A resolution. Nat Struct Biol *7*, 687-692.

Haug, G., Wilde, C., Leemhuis, J., Meyer, D. K., Aktories, K., and Barth, H. (2003). Cellular uptake of Clostridium botulinum C2 toxin: membrane translocation of a fusion toxin requires unfolding of its dihydrofolate reductase domain. Biochemistry *42*, 15284-15291.

Herreros, J., Lalli, G., Montecucco, C., and Schiavo, G. (2000). Tetanus toxin fragment C binds to a protein present in neuronal cell lines and motoneurons. J Neurochem *74*, 1941-1950.

Herreros, J., Ng, T., and Schiavo, G. (2001). Lipid Rafts Act as Specialized Domains for Tetanus Toxin Binding and Internalization into Neurons. Mol Biol Cell *12*, 2947-2960.

Hooper, N. M. (1999). Detergent-insoluble glycosphingolipid/cholesterol-rich membrane domains, lipid rafts and caveolae (review). Mol Membr Biol *16*, 145-156.

Hughes, R., and Whaler, B. C. (1962). Influence of nerve-ending activity and of drugs on the rate of paralysis of rat diaphragm preparations by Cl. botulinum type A toxin. J Physiol *160*, 221-233.

Humeau, Y., Doussau, F., Grant, N. J., and Poulain, B. (2000). How botulinum and tetanus neurotoxins block neurotransmitter release. Biochimie *82*, 427-446.

Ishitsuka, R., Yamaji-Hasegawa, A., Makino, A., Hirabayashi, Y., and Kobayashi, T. (2004). A Lipid-Specific Toxin Reveals Heterogeneity of Sphingomyelin-Containing Membranes. Biophys J *86*, 296-307.

Jahn, R., Lang, T., and Sudhof, T. C. (2003). Membrane fusion. Cell *112*, 519-533.

Jankovic, J. (2006). Botulinum toxin therapy for cervical dystonia. Neurotox Res *9*, 145-148.

Jankovic, J., and Schwartz, K. (1995). Response and immunoresistance to botulinum toxin injections. Neurology *45*, 1743-1746.

Jin, R., Rummel, A., Binz, T., and Brunger, A. T. (2006). Botulinum neurotoxin B recognizes its protein receptor with high affinity and specificity. Nature *444*, 1092-1095.

Jin, Y., Mozsolits, H., Hammer, J., Zmuda, E., Zhu, F., Zhang, Y., Aguilar, M. I., and Blazyk, J. (2003). Influence of tryptophan on lipid binding of linear amphipathic cationic antimicrobial peptides. Biochemistry *42*, 9395-9405.

Jurasinski, C. V., Lieth, E., Dang Do, A. N., and Schengrund, C. L. (2001). Correlation of cleavage of SNAP-25 with muscle function in a rat model of Botulinum neurotoxin type A induced paralysis. Toxicon *39*, 1309-1315.

Keller, J. E., Cai, F., and Neale, E. A. (2004). Uptake of botulinum neurotoxin into cultured neurons. Biochemistry *43*, 526-532.

Kielian, M., and Rey, F. A. (2006). Virus membrane-fusion proteins: more than one way to make a hairpin. Nat Rev Microbiol *4*, 67-76.

Kinoshita, M. (2008). Intermolecular interaction of phosphatidylinositol with the lipid raft molecules sphingomyelin and cholesterol. Biophysics *Vol. 4*, 1-9.

Kitamura, M., Igimi, S., Furukawa, K., and Furukawa, K. (2005). Different response of the knockout mice lacking b-series gangliosides against botulinum and tetanus toxins. Biochim Biophys Acta *1741*, 1-3.

Kiyokawa, E., Baba, T., Otsuka, N., Makino, A., Ohno, S., and Kobayashi, T. (2005). Spatial and Functional Heterogeneity of Sphingolipid-rich Membrane Domains. J Biol Chem *280*, 24072-24084.

Kurazono, H., Mochida, S., Binz, T., Eisel, U., Quanz, M., Grebenstein, O., Wernars, K., Poulain, B., Tauc, L., and Niemann, H. (1992). Minimal essential domains specifying toxicity of the light chains of tetanus toxin and botulinum neurotoxin type A. J Biol Chem *267*, 14721-14729.

Kutateladze, T., and Overduin, M. (2001). Structural mechanism of endosome docking by the FYVE domain. Science *291*, 1793-1796.

Kwiatkowska, K., Hordejuk, R., Szymczyk, P., Kulma, M., Abdel-Shakor, A.-B., lstrok, ucienniczak, A., Do, lstrok, owy, K., *et al.* (2007). Lysenin-His, a sphingomyelin-recognizing toxin, requires tryptophan 20 for cation-selective channel assembly but not for membrane binding. Molecular Membrane Biology *99999*, 1 - 14.

Lacy, D. B., and Stevens, R. C. (1999). Sequence homology and structural analysis of the clostridial neurotoxins. J Mol Biol *291*, 1091-1104.

Lacy, D. B., Tepp, W., Cohen, A. C., DasGupta, B. R., and Stevens, R. C. (1998). Crystal structure of botulinum neurotoxin type A and implications for toxicity. Nat Struct Biol *5*, 898-902.

Lai, E. C. (2003). Lipid rafts make for slippery platforms. J Cell Biol *162*, 365-370.

Lalli, G., Bohnert, S., Deinhardt, K., Verastegui, C., and Schiavo, G. (2003). The journey of tetanus and botulinum neurotoxins in neurons. Trends in Microbiology *11*, 431-437.

Levy, R., Forsyth, C. M., LaPorte, S. L., Geren, I. N., Smith, L. A., and Marks, J. D. (2007). Fine and domain-level epitope mapping of botulinum neurotoxin type A neutralizing antibodies by yeast surface display. J Mol Biol *365*, 196-210.

Lew, M. F., Adornato, B. T., Duane, D. D., Dykstra, D. D., Factor, S. A., Massey, J. M., Brin, M. F., Jankovic, J., Rodnitzky, R. L., Singer, C., *et al.* (1997). Botulinum toxin type B: a double-blind, placebo-controlled, safety and efficacy study in cervical dystonia. Neurology *49*, 701-707.

Li, L., Binz, T., Niemann, H., and Singh, B. R. (2000). Probing the mechanistic role of glutamate residue in the zinc-binding motif of type A botulinum neurotoxin light chain. Biochemistry *39*, 2399-2405.

Lin, H. H., Han, L. Y., Zhang, H. L., Zheng, C. J., Xie, B., and Chen, Y. Z. (2006). Prediction of the functional class of lipid binding proteins from sequence-derived properties irrespective of sequence similarity. J Lipid Res *47*, 824-831.

Maget-Dana, R. (1999). The monolayer technique: a potent tool for studying the interfacial properties of antimicrobial and membrane-lytic peptides and their interactions

with lipid membranes. Biochimica et Biophysica Acta (BBA) - Biomembranes *1462*, 109-140.

Mahrhold, S., Rummel, A., Bigalke, H., Davletov, B., and Binz, T. (2006). The synaptic vesicle protein 2C mediates the uptake of botulinum neurotoxin A into phrenic nerves. FEBS Lett *580*, 2011-2014.

Martin, T. F. (2000). Racing lipid rafts for synaptic-vesicle formation. Nat Cell Biol *2*, E9-11.

Maruta, T., Dolimbek, B. Z., Aoki, K. R., Steward, L. E., and Atassi, M. Z. (2004). Mapping of the Synaptosome-Binding Regions on the Heavy Chain of Botulinum Neurotoxin A By Synthetic Overlapping Peptides Encompassing the Entire Chain. The Protein Journal *23*, 539-552.

Matteoli, M., Verderio, C., Rossetto, O., Iezzi, N., Coco, S., Schiavo, G., and Montecucco, C. (1996). Synaptic vesicle endocytosis mediates the entry of tetanus neurotoxin into hippocampal neurons. Proc Natl Acad Sci U S A *93*, 13310-13315.

Mezaki, T., Kaji, R., Kohara, N., Fujii, H., Katayama, M., Shimizu, T., Kimura, J., and Brin, M. F. (1995). Comparison of therapeutic efficacies of type A and F botulinum toxins for blepharospasm: a double-blind, controlled study. Neurology *45*, 506-508.

Montecucco, C. (1986). How do tetanus and botulinum toxins bind to neuronal membranes? . Trends in Biochemical Sciences *11(8)*, 314-317.

Montecucco, C., and Molgo, J. (2005). Botulinal neurotoxins: revival of an old killer. Curr Opin Pharmacol *5*, 274-279.

Montecucco, C., Papini, E., and Schiavo, G. (1994). Bacterial protein toxins penetrate cells via a four-step mechanism. FEBS Lett *346*, 92-98.

Montecucco, C., Rossetto, O., and Schiavo, G. (2004). Presynaptic receptor arrays for clostridial neurotoxins. Trends Microbiol *12*, 442-446.

Montecucco, C., and Schiavo, G. (1995). Structure and function of tetanus and botulinum neurotoxins. Q Rev Biophys *28*, 423-472.

Montecucco, C., Schiavo, G., and Dasgupta, B. R. (1989). Effect of pH on the interaction of botulinum neurotoxins A, B and E with liposomes. Biochem J *259*, 47-53.

Montecucco, C., Schiavo, G., Tugnoli, V., and de Grandis, D. (1996). Botulinum neurotoxins: mechanism of action and therapeutic applications. Mol Med Today *2*, 418-424.

Morbiato, L., Carli, L., Johnson, E. A., Montecucco, C., Molgo, J., and Rossetto, O. (2007). Neuromuscular paralysis and recovery in mice injected with botulinum neurotoxins A and C. Eur J Neurosci *25*, 2697-2704.

Naumann, M., and Jost, W. (2004). Botulinum toxin treatment of secretory disorders. Mov Disord *19 Suppl 8*, S137-141.

Nishiki, T., Kamata, Y., Nemoto, Y., Omori, A., Ito, T., Takahashi, M., and Kozaki, S. (1994). Identification of protein receptor for Clostridium botulinum type B neurotoxin in rat brain synaptosomes. J Biol Chem *269*, 10498-10503.

Nishiki, T., Tokuyama, Y., Kamata, Y., Nemoto, Y., Yoshida, A., Sato, K., Sekiguchi, M., Takahashi, M., and Kozaki, S. (1996). The high-affinity binding of Clostridium

botulinum type B neurotoxin to synaptotagmin II associated with gangliosides GT1b/GD1a. FEBS Lett *378*, 253-257.

Osen-Sand, A., Staple, J. K., Naldi, E., Schiavo, G., Rossetto, O., Petitpierre, S., Malgaroli, A., Montecucco, C., and Catsicas, S. (1996). Common and distinct fusion proteins in axonal growth and transmitter release. J Comp Neurol *367*, 222-234.

Pellizzari, R., Mason, S., Shone, C. C., and Montecucco, C. (1997). The interaction of synaptic vesicle-associated membrane protein/synaptobrevin with botulinum neurotoxins D and F. FEBS Lett *409*, 339-342.

Pellizzari, R., Rossetto, O., Lozzi, L., Giovedi, S., Johnson, E., Shone, C. C., and Montecucco, C. (1996). Structural determinants of the specificity for synaptic vesicle-associated membrane protein/synaptobrevin of tetanus and botulinum type B and G neurotoxins. J Biol Chem *271*, 20353-20358.

Pike, L. J. (2004). Lipid rafts: heterogeneity on the high seas. Biochem J *378*, 281-292.

Puhar, A., Johnson, E. A., Rossetto, O., and Montecucco, C. (2004). Comparison of the pH-induced conformational change of different clostridial neurotoxins. Biochem Biophys Res Commun *319*, 66-71.

Raciborska, D. A., Trimble, W. S., and Charlton, M. P. (1998). Presynaptic protein interactions in vivo: evidence from botulinum A, C, D and E action at frog neuromuscular junction. Eur J Neurosci *10*, 2617-2628.

Ratts, R., Zeng, H., Berg, E. A., Blue, C., McComb, M. E., Costello, C. E., vanderSpek, J. C., and Murphy, J. R. (2003). The cytosolic entry of diphtheria toxin catalytic domain requires a host cell cytosolic translocation factor complex. J Cell Biol *160*, 1139-1150.

Rigoni, M., Caccin, P., Johnson, E. A., Montecucco, C., and Rossetto, O. (2001). Site-directed mutagenesis identifies active-site residues of the light chain of botulinum neurotoxin type A. Biochem Biophys Res Commun *288*, 1231-1237.

Rossetto, O., Caccin, P., Rigoni, M., Tonello, F., Bortoletto, N., Stevens, R. C., and Montecucco, C. (2001a). Active-site mutagenesis of tetanus neurotoxin implicates TYR-375 and GLU-271 in metalloproteolytic activity. Toxicon *39*, 1151-1159.

Rossetto, O., and Montecucco, C. (2007). Peculiar binding of botulinum neurotoxins. ACS Chem Biol *2*, 96-98.

Rossetto, O., Morbiato, L., Caccin, P., Rigoni, M., and Montecucco, C. (2006). Presynaptic enzymatic neurotoxins. J Neurochem *97*, 1534-1545.

Rossetto, O., Schiavo, G., Montecucco, C., Poulain, B., Deloye, F., Lozzi, L., and Shone, C. C. (1994). SNARE motif and neurotoxins. Nature *372*, 415-416.

Rossetto, O., Seveso, M., Caccin, P., Schiavo, G., and Montecucco, C. (2001b). Tetanus and botulinum neurotoxins: turning bad guys into good by research. Toxicon *39*, 27-41.

Roux, S., Colasante, C., Saint Cloment, C., Barbier, J., Curie, T., Girard, E., Molgo, J., and Brulet, P. (2005). Internalization of a GFP-tetanus toxin C-terminal fragment fusion protein at mature mouse neuromuscular junctions. Mol Cell Neurosci *30*, 79-89.

Rummel, A., Bade, S., Alves, J., Bigalke, H., and Binz, T. (2003). Two carbohydrate binding sites in the H(CC)-domain of tetanus neurotoxin are required for toxicity. J Mol Biol *326*, 835-847.

Rummel, A., Eichner, T., Weil, T., Karnath, T., Gutcaits, A., Mahrhold, S., Sandhoff, K., Proia, R. L., Acharya, K. R., Bigalke, H., and Binz, T. (2007). Identification of the protein receptor binding site of botulinum neurotoxins B and G proves the double-receptor concept. Proc Natl Acad Sci U S A *104*, 359-364.

Rummel, A., Karnath, T., Henke, T., Bigalke, H., and Binz, T. (2004a). Synaptotagmins I and II act as nerve cell receptors for botulinum neurotoxin G. J Biol Chem *279*, 30865-30870.

Rummel, A., Mahrhold, S., Bigalke, H., and Binz, T. (2004b). The HCC-domain of botulinum neurotoxins A and B exhibits a singular ganglioside binding site displaying serotype specific carbohydrate interaction. Mol Microbiol *51*, 631-643.

Sankhla, C., Jankovic, J., and Duane, D. (1998). Variability of the immunologic and clinical response in dystonic patients immunoresistant to botulinum toxin injections. Mov Disord *13*, 150-154.

Schiavo, G. (2006). Structural biology: Dangerous liaisons on neurons. Nature *444*, 1019-1020.

Schiavo, G., Demel, R., and Montecucco, C. (1991). On the role of polysialoglycosphingolipids as tetanus toxin receptors. A study with lipid monolayers. Eur J Biochem *199*, 705-711.

Schiavo, G., Matteoli, M., and Montecucco, C. (2000). Neurotoxins affecting neuroexocytosis. Physiol Rev *80*, 717-766.

Scott, A. B., Magoon, E. H., McNeer, K. W., and Stager, D. R. (1989). Botulinum treatment of strabismus in children. Trans Am Ophthalmol Soc *87*, 174-180; discussion 180-174.

Segelke, B., Knapp, M., Kadkhodayan, S., Balhorn, R., and Rupp, B. (2004). Crystal structure of Clostridium botulinum neurotoxin protease in a product-bound state: Evidence for noncanonical zinc protease activity. Proc Natl Acad Sci U S A *101*, 6888-6893.

Shaner, N. C., Campbell, R. E., Steinbach, P. A., Giepmans, B. N. G., Palmer, A. E., and Tsien, R. Y. (2004). Improved monomeric red, orange and yellow fluorescent proteins derived from Discosoma sp. red fluorescent protein. Nat Biotech *22*, 1567-1572.

Simpson, L. L., Coffield, J. A., and Bakry, N. (1994). Inhibition of vacuolar adenosine triphosphatase antagonizes the effects of clostridial neurotoxins but not phospholipase A2 neurotoxins. J Pharmacol Exp Ther *269*, 256-262.

Sloop, R. R., Cole, B. A., and Escutin, R. O. (1997). Human response to botulinum toxin injection: type B compared with type A. Neurology *49*, 189-194.

Sudhof, T. C. (2004). The synaptic vesicle cycle. Annu Rev Neurosci *27*, 509-547.

Swaminathan, S., and Eswaramoorthy, S. (2000). Structural analysis of the catalytic and binding sites of Clostridium botulinum neurotoxin B. Nat Struct Biol *7*, 693-699.

Sweeney, S. T., Broadie, K., Keane, J., Niemann, H., and O'Kane, C. J. (1995). Targeted expression of tetanus toxin light chain in Drosophila specifically eliminates synaptic transmission and causes behavioral defects. Neuron *14*, 341-351.

Tacket, C. O., Rogawski MA (1989). Botulism. In: Simpson L. L (ed) Botulinum neurotoxins and tetanus toxin. Academic Press, San Diego, CA,, pp 351–378.

Thesleff, S. (1960). Supersensitivity of skeletal muscle produced by botulinum toxin. J Physiol *151*, 598-607.

Truong, D. D., and Jost, W. H. (2006). Botulinum toxin: clinical use. Parkinsonism Relat Disord *12*, 331-355.

Tsukamoto, K., Kohda, T., Mukamoto, M., Takeuchi, K., Ihara, H., Saito, M., and Kozaki, S. (2005). Binding of Clostridium botulinum type C and D neurotoxins to ganglioside and phospholipid. Novel insights into the receptor for clostridial neurotoxins. J Biol Chem *280*, 35164-35171.

Tsukamoto, K., Kozai, Y., Ihara, H., Kohda, T., Mukamoto, M., Tsuji, T., and Kozaki, S. (2008). Identification of the receptor-binding sites in the carboxyl-terminal half of the heavy chain of botulinum neurotoxin types C and D. Microb Pathog *44*, 484-493.

Turton, K., Chaddock, J. A., and Acharya, K. R. (2002). Botulinum and tetanus neurotoxins: structure, function and therapeutic utility. Trends in Biochemical Sciences *27*, 552-558.

Vaidyanathan, V. V., Yoshino, K., Jahnz, M., Dorries, C., Bade, S., Nauenburg, S., Niemann, H., and Binz, T. (1999). Proteolysis of SNAP-25 isoforms by botulinum neurotoxin types A, C, and E: domains and amino acid residues controlling the formation of enzyme-substrate complexes and cleavage. J Neurochem *72*, 327-337.

Vicinanza, M., D'Angelo, G., Di Campli, A., and De Matteis, M. A. (2008). Function and dysfunction of the PI system in membrane trafficking. Embo J *27*, 2457-2470.

Washbourne, P., Pellizzari, R., Baldini, G., Wilson, M. C., and Montecucco, C. (1997). Botulinum neurotoxin types A and E require the SNARE motif in SNAP-25 for proteolysis. FEBS Lett *418*, 1-5.

Weissenhorn, W., Dessen, A., Harrison, S. C., Skehel, J. J., and Wiley, D. C. (1997). Atomic structure of the ectodomain from HIV-1 gp41. Nature *387*, 426-430.

Williamson, L. C., Halpern, J. L., Montecucco, C., Brown, J. E., and Neale, E. A. (1996). Clostridial neurotoxins and substrate proteolysis in intact neurons: botulinum neurotoxin C acts on synaptosomal-associated protein of 25 kDa. J Biol Chem *271*, 7694-7699.

Yamaji, A., Sekizawa, Y., Emoto, K., Sakuraba, H., Inoue, K., Kobayashi, H., and Umeda, M. (1998). Lysenin, a Novel Sphingomyelin-specific Binding Protein. J Biol Chem *273*, 5300-5306.

Yamasaki, S., Hu, Y., Binz, T., Kalkuhl, A., Kurazono, H., Tamura, T., Jahn, R., Kandel, E., and Niemann, H. (1994). Synaptobrevin/vesicle-associated membrane protein (VAMP) of Aplysia californica: structure and proteolysis by tetanus toxin and botulinal neurotoxins type D and F. Proc Natl Acad Sci U S A *91*, 4688-4692.

Yowler, B. C., Kensinger, R. D., and Schengrund, C. L. (2002). Botulinum neurotoxin A activity is dependent upon the presence of specific gangliosides in neuroblastoma cells expressing synaptotagmin I. J Biol Chem *277*, 32815-32819.

Zuber, M., Sebald, M., Bathien, N., de Recondo, J., and Rondot, P. (1993). Botulinum antibodies in dystonic patients treated with type A botulinum toxin: frequency and significance. Neurology *43*, 1715-1718.